AN ABSTRACT OF THE DISSERTATION OF

Paul Logan for the degree of Doctor of Philosophy in Statistics presented on March 16, 2020.

Title: C-SHIFT, Quantile Theory, and Assessing Monotonicity

Abstract approved: _____

Debashis Mondal Yevgeniy Kovchegov

DNA microarray technology is a powerful tool for analyzing patterns in gene expression data for thousands of genes. Due to a number of systematic variations in microarray experiments, the raw gene expression data is often obfuscated by undesirable technical noises. Various normalization techniques were designed in an attempt to remove these non-biological errors prior to any statistical analysis. One of the reasons for normalizing data is the need for recovering the covariance matrix used in gene network analysis. We introduce and demonstrate a novel normalization technique, called the covariance shift (C-SHIFT) method. We prove that under certain conditions applying quantile normalization prior to performing Welch's t-test can increase the value of the test statistics. We discuss the probabilistic monotonicity property of covariance graph models through a set of mean and correlation inequalities. Our analysis suggests that for two different studies, comprising healthy and cervical cancer patients, underlying biological networks

largely follow the probabilistic monotonicity property.

C-SHIFT, Quantile Theory, and Assessing Monotonicity

by

Paul Logan

A DISSERTATION

submitted to

Oregon State University

in partial fulfillment of
the requirements for the
degree of

Doctor of Philosophy

Presented March 16, 2020
Commencement June 2020

Doctor of Philosophy dissertation of Paul Logan presented on March 16, 2020.

APPROVED:

Co-Major Professor, representing Statistics

Co-Major Professor, representing Statistics

Chair of the Department of Statistics

Dean of the Graduate School

I understand that my dissertation will become part of the permanent collection of Oregon State University libraries. My signature below authorizes release of my dissertation to any reader upon request.

Paul Logan, Author

ACKNOWLEDGEMENTS

I would like to acknowledge Evgenia Chunikhina for her extensive work on the C-Shift algorithm discussed in this Thesis. I would like to thank Andrey Morgun and Anatoly Yambartsev for contributing their expertise. I would like to thank Sharmodeep Bhattacharyya, Ren Guo, and Duo Jiang for serving on my committee. I would like to thank Michael Dumelle, Chris Skypeck, and Miao Yang for productive conversations. I would like to thank my wife, Amber Logan, for her patience, understanding, and support. Finally, I would like to thank my advisors Yevgeniy Kovchegov and Debashis Mondal for their knowledge and guidance.

This research was supported by NSF awards DMS-1412557 and DMS-1519890.

TABLE OF CONTENTS

TABLE OF CONTENTS (Continued)

LIST OF FIGURES

LIST OF FIGURES (Continued)

LIST OF TABLES

LIST OF ALGORITHMS

C-SHIFT, Quantile Theory, and Assessing Monotonicity

1 Introduction

DNA microarray technology is a powerful tool for analyzing patterns in gene expression data for thousands of genes. Due to a number of systematic variations in microarray experiments, the raw gene expression data is often obfuscated by undesirable technical noises. Various normalization techniques were designed in an attempt to remove these non-biological errors prior to any statistical analysis. One of the reasons for normalizing data is the need for recovering the covariance matrix used in gene network analysis.

In the first chapter we introduce a novel normalization technique, called the covariance shift (C-SHIFT) method. This normalization algorithm uses optimization techniques together with the blessing of dimensionality philosophy and an energy minimization hypothesis for covariance matrix recovery under additive noise (in biology, known as the bias). Thus, it is perfectly suited for the analysis of logarithmic gene expressions data. Numerical experiments on synthetic data demonstrate the method's advantage over the classical normalization techniques. Namely, the comparison is made with rank, quantile, cyclic LOESS (locally estimated scatterplot smoothing), and MAD (median absolute deviation) normalization methods.

In the second chapter, we examine the impact of quantile normalization on the t-test in statistics of gene data. We prove that under certain conditions, even

in the noiseless environment, applying quantile normalization prior to performing Welch's t-test can increase the value of the test statistics.

In the third chapter, we discuss the probabilistic monotonicity property of covariance graph models. The focus here is on biological networks that transit from one state to another. Typically, monotonicity arises in the context of causal interpretation. For a pair of covariance graphs, it is shown that the monotonicity leads to a set of mean and correlation inequalities. Statistical tests with multiplicity corrections can thus be applied to assess monotonicity, to control family-wise error rate and to select covariance graphs. Two applications are considered with gene expression data from two different studies comprising healthy and cervical cancer patients. The analysis suggests that for both studies underlying biological networks largely follow the probabilistic monotonicity property.

2 The covariance shift (C-SHIFT) algorithm for normalizing biological data

DNA microarray technology plays an important role in genomic research. This technology allows for the collection of massive amounts of simultaneous measurements of gene expression levels of thousands to tens of thousands of genes. Analyzing different patterns of gene expressions helps to gain insight into complex biological phenomena such as development, aging, onset and progression of diseases, and cellular response/reaction to drugs/treatments. Although DNA microarray technology has been extensively used in various genomic related studies, it is well known that this technique generates some technical noise which affects the measured gene expression levels [31, 57]. To extract accurate biological information it becomes necessary to normalize the data to filter out/compensate for these non-biological noises/errors. Normalization is a crucial pre-processing step in the microarray data analysis. The gene expression data will vary significantly after different normalization methods. Thus, the results of further data analysis (e.g. gene expression network) will be critically dependent on a choice of a normalization technique. A variety of normalization procedures have been used on microarray data sets. See [47, 53, 50, 5, 7, 44, 56] and reference therein for a review and comparison of current normalization strategies. In this chapter we develop a novel normalization technique, called the covariance shift (C-SHIFT) method, and com-

pare it to the following well known normalization methods used in microarray data analysis: rank, quantile, cyclic LOESS (locally estimated scatterplot smoothing), and MAD (median absolute deviation). See [48, 7, 1, 50] and references therein for more details on the above listed normalization methods.

Consider a situation where the gene expression data is subjected to multiplicative noise (aka bias). Specifically, let $X_n^{(i)}$ be the true gene expression, where subscript index n stands for the n-th gene in the network and the superscript index i stands for the i-th measurement. The observed gene expression, denoted by $\widetilde{X}_n^{(i)}$, is different from $X_n^{(i)}$ due to all gene expressions in the i-th measurement being distorted by i.i.d. multiplicative noise variable $W^{(i)}$, i.e.,

$$\widetilde{X}_n^{(i)} = W^{(i)} X_n^{(i)}. \tag{2.1}$$

Here, both the observed and the true gene expressions are positive, i.e., $X_n^{(i)} > 0$ and $W^{(i)} > 0$. The random variables $X_n^{(i)}$ are independent of the variable $W^{(i)}$.

In biology, the multiplicative noise $W^{(i)}$ is referred to as the bias. The bias is prompted by random events causing an error in the measurement of the total amount of RNA. Such random events are often related to different levels of tissue preservation in different sample that leads to variability of RNA degradation. Consequently, this leads to an RNA detection problem. Additionally, there are other technical reasons for an error in the measurement of the total amount of RNA in a given sample that may lead to a bias in (2.1). All other noise (e.g. misreading parts of RNA) goes into the variable $X_n^{(i)}$.

The multiplicative noise in (2.1) implies the corresponding additive noise (bias) in the logarithimic gene expression data:

$$\widetilde{Y}_n^{(i)} = Y_n^{(i)} + V^{(i)}, \tag{2.2}$$

where we let $\widetilde{Y}_n^{(i)} := \log \widetilde{X}_n^{(i)}$, $Y_n^{(i)} := \log X_n^{(i)}$, and $V^{(i)} := \log W^{(i)}$.

The bias, whether multiplicative as in (2.1) or additive as in (2.2), causes the correlations to be shifted away from -1. Indeed, since

$$\begin{aligned} \operatorname{Cov}(\widetilde{X}_n, \widetilde{X}_m) = {} & \operatorname{E}[W^2] \operatorname{Cov}(X_n, X_m) \\ & + \operatorname{Var}(W) \operatorname{E}[X_n] \operatorname{E}[X_m] \end{aligned} \tag{2.3}$$

the correlation of observed gene expressions

$$\begin{aligned} & corr(\widetilde{X}_n, \widetilde{X}_m) \\ & = \frac{\operatorname{Cov}(X_n, X_m) + \nu \operatorname{E}[X_n] \operatorname{E}[X_m]}{\sqrt{(\operatorname{Var}(X_n) + \nu E^2[X_n])(\operatorname{Var}(X_m) + \nu E^2[X_m])}}, \end{aligned} \tag{2.4}$$

where $\nu := \frac{\operatorname{Var}(W)}{\operatorname{E}[W^2]} > 0$. Notice that if $\operatorname{Cov}(X_n, X_m)$ is negative, by adding positive multiples of $\nu > 0$ in the numerator and the denominator as in (2.4), we arrive at $corr(\widetilde{X}_n, \widetilde{X}_m) > corr(X_n, X_m)$. In other words, all negative correlations $corr(X_n, X_m)$ will either turn into positive, or negative of smaller magnitude in the observed variables $\widetilde{X}_n$. While the multiplicative bias $W^{(i)} \approx 1$ (similarly, the additive bias $V^{(i)} \approx 0$) may not appear critical, they are known to cause significant

problems in gene correlation structure analyses. Specifically, this phenomenon is known to cause the disappearance of the large magnitude negative correlations in the observed biological data, $\widetilde{X}_n$, which hampers the ability to perform certain types of statistical data analysis, such as the false discovery rate (FDR) method.

The same is observed for the logarithmic data (2.2). Similarly to (2.3), the independent additive noise in (2.2) implies an increase of covariance,

$$\mathrm{Cov}(\widetilde{Y}_n, \widetilde{Y}_m) = \mathrm{Cov}(Y_n, Y_m) + \omega, \tag{2.5}$$

where $\omega = \mathrm{Var}(V) > 0$. Consequently, the correlations in the logarithmic data are

$$corr(\widetilde{Y}_n, \widetilde{Y}_m) = \frac{\mathrm{Cov}(Y_n, Y_m) + \omega}{\sqrt{\Big(\mathrm{Var}(Y_n) + \omega\Big)\Big(\mathrm{Var}(Y_m) + \omega\Big)}}. \tag{2.6}$$

Here too, if $\mathrm{Cov}(Y_n, Y_m)$ is negative, by adding $\omega > 0$ in the numerator and the denominator, we obtain

$$corr(\widetilde{Y}_n, \widetilde{Y}_m) > corr(Y_n, Y_m).$$

Thus, the phenomenon of disappearance of the large magnitude negative correlations also applies to the logarithmic data $\widetilde{Y}_n$.

Denote by $\widehat{\mathrm{Cov}}$ the empirical covariances taken over N subjects for each of $\binom{M}{2}$ pairs of genes. Similarly, let $\widehat{\mathrm{Var}}$ denote the empirical variance. Then, equation

(2.2) yields the observed empirical covariance

$$\widehat{\mathrm{Cov}}(\widetilde{Y}_n, \widetilde{Y}_m) = \widehat{\mathrm{Cov}}(Y_n, Y_m) - \hat{a}_n - \hat{a}_m + \hat{\omega} \tag{2.7}$$

for all pairs of gene indices n and m, where $\hat{a}_n = \widehat{\mathrm{Cov}}(Y_n, V)$ for all $n = 1, \ldots, M$, and $\hat{\omega} = \widehat{\mathrm{Var}}(V) > 0$. As is often the case, $\hat{\omega}$ can be very large relative to the values of $\hat{a}_n$, causing the disappearance of the large magnitude negative correlations in empirical data.

The goal of the covariance shift (C-SHIFT) normalization method introduced here is the recovery of the true empirical covariances $\widehat{\mathrm{Cov}}(Y_n, Y_m)$ and the respective true empirical correlations in the case of the logarithmic gene expression data or any other situations with additive noise as in (2.2).

Let $\widetilde{C} = \big(\widehat{\mathrm{Cov}}(\widetilde{Y}_n, \widetilde{Y}_m)\big)_{n,m}$ be the empirical covariance matrix of the observed data $\widetilde{Y}_n^{(i)}$, and let $C = \Big(\widehat{\mathrm{Cov}}(Y_n, Y_m)\Big)_{n,m}$ be the empirical covariance matrix of the cleaned data $Y_n^{(i)}$ (i.e., the true empirical covariance) that we desire to recover. Formula (2.7) rewritten in the matrix form states

$$C = \widetilde{C} + \hat{a}\mathbf{1}^T + \mathbf{1}^T\hat{a} - \hat{\omega}\,\mathbf{1}\mathbf{1}^T, \tag{2.8}$$

where $\hat{a} = \big(\hat{a}_1, \ldots, \hat{a}_M\big)^T$, and $\mathbf{1}$ denotes the column vector of 1's, hence $\mathbf{1}\mathbf{1}^T$ is a square matrix of 1's.

Our goal here is to estimate $\hat{a}$ and $\hat{\omega}$ in (2.8), and thus recover the true empirical covariance matrix C. This will be done in Section 2.1. We assume large dimension

M. There will be two cases.

Case I: If $\det(\widetilde{C}) = 0$ (e.g. $N < M$), we make a small perturbation of the diagonal entries of $\widetilde{C}$ (the variances) resulting in a new covariance matrix being positive definite whose smallest eigenvalue is still very close to zero. Next, we use energy minimization to estimate $\hat{a}_n$ and $\hat{\omega}$ in (2.8).

Case II: If $\widetilde{C}$ is positive definite, our approach exploits the phenomenon sometimes referred to as the *curse of dimensionality* [2, 51] and sometimes as the *blessing of dimensionality* [27, 16, 35], postulating that in higher dimensions almost all data points are located near extrema (i.e., in the outer shell)[1]. In other words, for large M, we anticipate the smallest eigenvalue of C to be near zero. As a rigorous bound, we observe that if some of the correlations $corr(Y_n, Y_m)$ are located in $[-1, \delta - 1]$ interval, then the smallest eigenvalue of C is located within $\left[0, \delta \min_n \widehat{\mathrm{Var}}(Y_n)\right]$ interval. Thus, as in Case I, under the blessing of dimensionality assumption, we again use energy minimization for estimating $\hat{a}_n$ and $\hat{\omega}$.

The problem of improving the existing and developing new normalization methods is very important for scientists working with biological data. The fact that normalization alters the data-correlation structure was stated in Saccenti [56]. Besides [56] gives a comprehensive overview of normalization methods. In Bolstad *et al.* [7] the authors compare three complete data normalization methods (cyclic loess, contrast based method, and quantile) that make use of data from all arrays in an experiment to two methods that make use of a baseline array. The comparison was

[1] In this chapter we will refer to the phenomenon as the blessing of dimensionality rather than the curse of dimensionality.

done on two publicly available datasets with the results favoring the complete data methods. For more on the normalization methods, see [1, 24, 31, 34, 50, 55, 61].

2.1 Theoretical derivations

Proposition 1. *Suppose $\mathcal{M}$ is a symmetric positive definite square matrix. Then,*

$$\begin{aligned} v^* &:= \max\left\{v :\ \mathcal{M} - v\,\mathbf{1}\mathbf{1}^T \ \textit{is positive semidefinite}\ \right\} \\ &= \frac{1}{\mathbf{1}^T\,\mathcal{M}^{-1}\,\mathbf{1}}. \end{aligned}$$

Proof. Observe that

$$x^T\big(\mathcal{M} - v\,\mathbf{1}\mathbf{1}^T\big)x = x^T\mathcal{M}x - v\left(\sum x_i\right)^2 \geq 0$$

for all $x \in \mathbb{R}^M$ if and only if $v \leq v^*$, where v^* minimizes $x^T\mathcal{M}x$ under the condition $\sum x_i = Const$. Next, applying the Lagrange multipliers method, we obtain $2\mathcal{M}x = \lambda\mathbf{1}$, and therefore,

$$v^* = \frac{x^T\mathcal{M}x}{(\sum x_i)^2} = \frac{\frac{\lambda}{2}x^T\mathbf{1}}{(\sum x_i)^2} = \frac{\lambda/2}{\mathbf{1}^T x} = \frac{1}{\mathbf{1}^T\,\mathcal{M}^{-1}\,\mathbf{1}}$$

as $x = \frac{\lambda}{2}\mathcal{M}^{-1}\mathbf{1}$. □

Suppose the empirical covariance matrix $\widetilde{C}$ is positive definite, i.e., $\widetilde{C}$ is of full rank. Consider values of a column vector $\alpha = (\alpha_1, \ldots, \alpha_M)^T$ such that $\widetilde{C} + \alpha\mathbf{1}^T + \mathbf{1}^T\alpha$ is

positive definite. Then, by Prop. 1,

$$C_\alpha := \widetilde{C} + \alpha \mathbf{1}^T + \mathbf{1}^T \alpha - v(\alpha) \mathbf{1}\mathbf{1}^T \tag{2.9}$$

is positive semidefinite with $\det(C_\alpha) = 0$, where we let

$$v(\alpha) := \frac{1}{\mathbf{1}^T \left(\widetilde{C} + \alpha \mathbf{1}^T + \mathbf{1}^T \alpha\right)^{-1} \mathbf{1}}. \tag{2.10}$$

Next, recall the quantities $\hat{a}$ and $\hat{w}$ in (2.8). If $\widetilde{C}$ is rank deficient, we perturb its diagonal entries by adding small positive (random or deterministic) values, and if $\widetilde{C}$ is positive definite, we assume the blessing of dimensionality phenomenon holds. Thus, in either case, we work under the assumption that $\widetilde{C}$ is positive definite with its smallest eigenvalue located near zero. Then, Prop. 1 implies $\hat{w} \approx v(\hat{a})$, where $v(\alpha)$ is as defined in (2.10). Therefore, letting $\alpha = \hat{a}$ in (2.9), we will have $C_{\hat{a}}$ approximating C.

Finally, for all $X \in \mathbb{R}^{M \times N}$, let $\|X\|_F$ denote the Frobenius norm of X and let $\mathcal{E}(X) = \frac{1}{2}\|X\|_F^2$ be the energy function. Our next assumption states that $\hat{a}$ can be estimated by the minimizer α^* of the energy function $\mathcal{E}(C_\alpha)$, i.e., we estimate $\hat{a}$ by

$$\alpha^* = \operatorname{argmin} \|C_\alpha\|_F.$$

The assumption is based on the observation that a random adjustment of the covariance via an additive noise (bias) as in (2.7) will result in an energy increase,

i.e., $\mathcal{E}(\widetilde{C}) > \mathcal{E}(C)$. Hence, C_{α^*} will approximate $C_{\hat{a}}$ and the desired true empirical covariance matrix C.

Lemma 1. *Suppose the empirical covariance matrix $\widetilde{C}$ is of full rank, and the quantities C_α and $v(\alpha)$ are as in* (2.9) *and* (2.10)*. Then, the gradient of the Frobenius norm squared is given by*

$$\begin{aligned}\frac{1}{4}\nabla\|C_\alpha\|_F^2 = M\alpha \\ &+ [M^2\, v^2(\alpha) - c\, v(\alpha) - 2Ma\, v(\alpha)]A_\alpha^{-1}\mathbf{1} \\ &+ \widetilde{C}\mathbf{1} + [a - M\, v(\alpha)]\mathbf{1}, \end{aligned} \tag{2.11}$$

where $\|\cdot\|_F$ denotes the Forbenius norm, and we let

$$A_\alpha := \widetilde{C} + \alpha\mathbf{1}^T + \mathbf{1}^T\alpha,$$

$c := \mathbf{1}^T\widetilde{C}\mathbf{1}$ *and* $a := \sum_{i=1}^{M} \alpha_i$.

Proof. By (2.9), we have

$$\begin{aligned}\|C_\alpha\|_F^2 =& \|\widetilde{C}\|_F^2 + 2M\sum_{i=1}^{M}\alpha_i^2 + M^2\, v^2(\alpha) + 4\left(\mathbf{1}^T\widetilde{C}\alpha\right) \\ &+ 2a^2 - 2c\, v(\alpha) - 4Ma\, v(\alpha) \end{aligned} \tag{2.12}$$

Notice that

$$\frac{\partial}{\partial \alpha_i} A_\alpha = \bar{e}_i \mathbf{1}^T + \mathbf{1}\bar{e}_i^T \quad \text{and}$$
$$\frac{\partial}{\partial \alpha_i} A_\alpha^{-1} = -A_\alpha^{-1}\left(\bar{e}_i \mathbf{1}^T + \mathbf{1}\bar{e}_i^T\right) A_\alpha^{-1}, \tag{2.13}$$

where $\bar{e}_i$ is the i-th coordinate vector. Therefore, we have

$$\begin{aligned}\frac{\partial}{\partial \alpha_i} v(\alpha) &= v^2(\alpha)\mathbf{1}^T A_\alpha^{-1}\left(\bar{e}_i \mathbf{1}^T + \mathbf{1}\bar{e}_i^T\right) A_\alpha^{-1}\,\mathbf{1} \\ &= 2v(\alpha)\,\mathbf{1}^T A_\alpha^{-1}\bar{e}_i \end{aligned} \tag{2.14}$$

implying

$$\nabla v(\alpha) = 2v(\alpha) A_\alpha^{-1}\mathbf{1}. \tag{2.15}$$

Next, the gradient $\nabla \|C_\alpha\|_F^2$ in (2.11) is found via the equations (2.12) and (2.15).

□

First, observe that C_α is invariant under the addition of multiples of $\mathbf{1}$ using the Sherman–Morrison formula. Thus, without loss of generality, we restrict the domain to a hyperplane $a = \text{Const}$. Next, observe that $\mathbf{1}^T \nabla \|C_\alpha\|_F^2 = 0$ in (2.11). Thus, in the gradient descent method, the value of a remains constant, i.e., throughout the algorithm, vector α remains on the same hyperplane $a = \text{Const}$.

Lemma 2. *Suppose the empirical covariance matrix $\widetilde{C}$ is of full rank, and the quantities C_α, $v(\alpha)$, and A_α are as in* (2.9), (2.10), *and* (2.12) *respectively. Then,*

the Hessian of $\|C_\alpha\|_F^2$*, denoted by* $H_\alpha := \mathrm{Hess}\big(\|C_\alpha\|_F^2\big)$ *is expressed as follows*

$$\begin{aligned}\frac{1}{4}H_\alpha =& MI + \mathbf{1}\mathbf{1}^T - 2M\, v(\alpha)\left(A_\alpha^{-1}\mathbf{1}\mathbf{1}^T + \mathbf{1}\mathbf{1}^T A_\alpha^{-1}\right)\\ &+ \left(3M^2\, v(\alpha) - c - 2Ma\right) v(\alpha) A_\alpha^{-1}\mathbf{1}\mathbf{1}^T A_\alpha^{-1}\\ &- \left(M^2\, v(\alpha) - c - 2Ma\right) A_\alpha^{-1}, \end{aligned} \tag{2.16}$$

where I *is the identity matrix,* $c = \mathbf{1}^T\widetilde{C}\mathbf{1}$*, and* $a = \sum_{i=1}^{M} \alpha_i$*.*

Proof. By (2.11), we have

$$\begin{aligned}\frac{1}{4}H_\alpha &= \frac{1}{4}\nabla\left(\nabla\|C_\alpha\|_F^2\right)^T\\ &= M\nabla\alpha^T\\ &+ \Big(\nabla\big(M^2\, v^2(\alpha) - c\, v(\alpha) - 2Ma\, v(\alpha)\big)\Big)\mathbf{1}^T A_\alpha^{-1}\\ &+ \big(M^2\, v^2(\alpha) - c\, v(\alpha) - 2Ma\, v(\alpha)\big)\nabla\mathbf{1}^T A_\alpha^{-1}\\ &+ \nabla\mathbf{1}^T\big(a - M\, v(\alpha)\big), \end{aligned} \tag{2.17}$$

where $\nabla = \left(\frac{\partial}{\partial\alpha_1}, \ldots, \frac{\partial}{\partial\alpha_M}\right)^T$ was used as the column vector of the partial derivative operators. The summation parts in (2.17) are calculated as follows. First,

$$M\nabla\alpha^T = MI. \tag{2.18}$$

Next, (2.15) implies

$$\begin{aligned}&\nabla\big(M^2\,v^2(\alpha)-c\,v(\alpha)-2Ma\,v(\alpha)\big)\\&\quad=2\big(2M^2\,v(\alpha)-c-2Ma\big)v(\alpha)A_\alpha^{-1}\mathbf{1}-2Mv(\alpha)\mathbf{1}.\end{aligned}\tag{2.19}$$

Equation (2.13) implies

$$\begin{aligned}\nabla\mathbf{1}^TA_\alpha^{-1}&=\sum_{i=1}^M\bar e_i\mathbf{1}^T\frac{\partial}{\partial\alpha_i}A_\alpha^{-1}\\&=-\sum_{i=1}^M\bar e_i\mathbf{1}^TA_\alpha^{-1}\left(\bar e_i\mathbf{1}^T+\mathbf{1}\bar e_i^T\right)A_\alpha^{-1}\\&=-\sum_{i=1}^M\left(\bar e_i^TA_\alpha^{-1}\mathbf{1}\right)\bar e_i\mathbf{1}^TA_\alpha^{-1}\\&\quad-\left(\mathbf{1}^TA_\alpha^{-1}\mathbf{1}\right)\sum_{i=1}^M\bar e_i\bar e_i^TA_\alpha^{-1}\\&=-A_\alpha^{-1}\mathbf{1}\mathbf{1}^TA_\alpha^{-1}-\left(\mathbf{1}^TA_\alpha^{-1}\mathbf{1}\right)A_\alpha^{-1}\\&=-A_\alpha^{-1}\mathbf{1}\mathbf{1}^TA_\alpha^{-1}-\frac{1}{v(\alpha)}A_\alpha^{-1}.\end{aligned}\tag{2.20}$$

Finally, (2.15) is used to derive

$$\nabla\mathbf{1}^T\big(a-M\,v(\alpha)\big)=\mathbf{1}\mathbf{1}^T-2M\,v(\alpha)A_\alpha^{-1}\mathbf{1}\mathbf{1}^T.\tag{2.21}$$

Combining together equations (2.18)-(2.21) and substituting them into (2.17) we obtain (2.16). □

Theorem 1. *Suppose the empirical covariance matrix $\widetilde{C}$ is of full rank, and the quantities C_α and $v(\alpha)$ are as in* (2.9) *and* (2.10)*. Then, the Frobenius norm squared $\|C_\alpha\|_F^2$ is convex, i.e.,*

$$\triangle\|C_\alpha\|_F^2 \geq 0 \quad \forall\alpha. \tag{2.22}$$

Proof. We will use the notations of this section such as $c := \mathbf{1}^T\widetilde{C}\mathbf{1}$ and $a := \sum_{i=1}^{M}\alpha_i$. Without loss of generality we consider α on the hyperplane $a = 0$.

Here, $A_\alpha = \widetilde{C} + \alpha\mathbf{1}^T + \mathbf{1}^T\alpha$ is a positive definite symmetric matrix with eigenvalues

$$\lambda_1 \geq \lambda_2 \geq \ldots \geq \lambda_M > 0$$

counted w.r.t. algebraic multiplicity, and let $\{v_i\}_{i=1,\ldots,M}$ be the corresponding orthonormal basis of eigenvectors.

Equation (2.16) implies

$$\begin{aligned}\frac{1}{4}\triangle\|C_\alpha\|_F^2 &= \frac{1}{4}\mathrm{Tr}\big(H_\alpha\big)\\ &= M^2\Big(1 - v(\alpha)\mathrm{Tr}\big(A_\alpha^{-1}\big)\Big)\\ &\quad + c\Big(\mathrm{Tr}\big(A_\alpha^{-1}\big) - v(\alpha)\mathbf{1}^T A_\alpha^{-2}\mathbf{1}\Big)\\ &\quad + 3M\Big(Mv^2(\alpha)\mathbf{1}^T A_\alpha^{-2}\mathbf{1} - 1\Big).\end{aligned} \tag{2.23}$$

The Laplacian in (2.23) is shown to be strictly positive in the following three steps.

First, by the Cauchy-Bunyakovsky-Schwarz inequality, we have

$$\begin{aligned} & Mv^2(\alpha)\mathbf{1}^T A_\alpha^{-2}\mathbf{1} - 1 \\ & \quad = v^2(\alpha)\Big(\|\mathbf{1}\|_2^2 \|A_\alpha^{-1}\mathbf{1}\|_2^2 - \big(\mathbf{1}^T A_\alpha^{-1}\mathbf{1}\big)^2\Big) \geq 0. \end{aligned} \tag{2.24}$$

Next, observe that for $M \geq 2$,

$$Mx + (1-x)^2 \geq 1 \quad \forall x \in [0,1].$$

Thus, for a given probability mass function $\{p_k\}_{k=1,\ldots,M}$ and index $i \in \{1,\ldots,M\}$, Jensen's inequality implies

$$\begin{aligned} & Mp_i + \left(\sum_{j:j\neq i} \lambda_j^{-1} p_j\right)\left(\sum_{j:j\neq i} \lambda_j p_j\right) \\ & \quad = Mp_i + (1-p_i)^2 \left(\sum_{j:j\neq i} \lambda_j^{-1} q_j\right)\left(\sum_{j:j\neq i} \lambda_j q_j\right) \\ & \quad \geq Mp_i + (1-p_i)^2 \ \geq 1 \end{aligned} \tag{2.25}$$

where we let $q_j = \frac{p_j}{1-p_i}$ for all $j \neq i$. Summing over all i in (2.25), we obtain,

$$\begin{aligned} \sum_i \lambda_i^{-1} p_i + \frac{1}{M}\sum_i \lambda_i^{-1}\left(\sum_{j:j\neq i} \lambda_j^{-1} p_j\right)\left(\sum_{j:j\neq i} \lambda_j p_j\right) \\ \geq \frac{1}{M}\sum_i \lambda_i^{-1}. \end{aligned} \tag{2.26}$$

Eqn. (2.26) implies

$$\sum_i \lambda_i^{-1} p_i + \frac{1}{M} \sum_i \lambda_i^{-1} p_i \left(\sum_{j:j\neq i} \lambda_j^{-1} \right) \left(\sum_k \lambda_k p_k \right) \geq \frac{1}{M} \sum_i \lambda_i^{-1}. \tag{2.27}$$

which rewrites as

$$\sum_i \lambda_i^{-1} p_i + \frac{1}{M} \left(\sum_i \lambda_i^{-1} p_i \right) \left(\sum_j \lambda_j^{-1} \right) \left(\sum_k \lambda_k p_k \right) \geq \frac{1}{M} \left(\sum_i \lambda_i^{-2} p_i \right) \left(\sum_k \lambda_k p_k \right) + \frac{1}{M} \sum_i \lambda_i^{-1}. \tag{2.28}$$

Finally, we let $p_i = \frac{1}{M}\big(\mathbf{1}^T v_i\big)^2$ and substitute the following expressions into (2.28):

$$\sum_i \lambda_i p_i = \frac{1}{M} \mathbf{1}^T A_\alpha \mathbf{1} = \frac{1}{M} \mathbf{1}^T \widetilde{C} \mathbf{1} = \frac{c}{M} \quad \text{as} \quad a = 0,$$

$$\sum_i \lambda_i^{-1} p_i = \frac{1}{M} \mathbf{1}^T A_\alpha^{-1} \mathbf{1} = \frac{1}{M\, v(\alpha)},$$

$$\sum_i \lambda_i^{-1} = \mathrm{Tr}\big(A_\alpha^{-1}\big), \quad \text{and} \quad \sum_i \lambda_i^{-2} p_i = \frac{1}{M} \mathbf{1}^T A_\alpha^{-2} \mathbf{1}.$$

Consequently, (2.28) rewrites as

$$M^2 \Big(1 - v(\alpha) \mathrm{Tr}\big(A_\alpha^{-1}\big)\Big) + c\Big(\mathrm{Tr}\big(A_\alpha^{-1}\big) - v(\alpha) \mathbf{1}^T A_\alpha^{-2} \mathbf{1}\Big) \geq 0. \tag{2.29}$$

Substituting (2.24) and (2.29) into (2.23), we then obtain $\triangle\|C_\alpha\|_F^2 \geq 0$. $\square$

2.1.1 Trace as alternative

An alternative version of the C-SHIFT algorithm is based on trace minimization. This is inspired by the statement of Proposition 1 and its eigenvalue interpretation. In this alternative C-SHIFT algorithm, the positive semi-definite matrix C_{α^*} with

$$\alpha^* = \operatorname{argmin} \operatorname{Tr}\big(C_\alpha\big)$$

is used to approximate the true empirical covariance matrix C. Empirically it appears that this alternative approach produces the same α^* as the original C-SHIFT algorithm based on Frobenius Norm minimization as presented in this chapter, and therefore it recovers the empirical covariance C with the same accuracy. Thus, the alternative, trace minimizing C-SHIFT algorithm can be used instead of Algorithm 1. In this subsection, we demonstrate an equivalent theoretical basis as already shown for the Frobenius norm as an objective function.

For all $X \in \mathbb{R}^{M\times N}$, let $\operatorname{Tr}(X)$ denote the trace of X. If X is symmetric and positive definite, and thus has a symmetric square root, $X^{1/2}$, then $\operatorname{Tr}(X) = \operatorname{Tr}(X^{1/2}X^{1/2}) = \|X^{1/2}\|_F^2$ is an energy function. Observe that a random adjustment of covariance by additive noise as in (2.7) will result in an energy increase, i.e., $\operatorname{Tr}(\widetilde{C}) > \operatorname{Tr}(C)$. Thus, we assume $\hat{a}$ can be estimated by

$$\alpha^* = \operatorname{argmin}\ \operatorname{Tr}\big(C_\alpha\big).$$

Hence, C_{α^*} will approximate $C_{\hat{a}}$ and thus C.

Lemma 3. *Suppose the empirical covariance matrix $\widetilde{C}$ is of full rank, and the quantities C_α and $v(\alpha)$ are as in* (2.9) *and* (2.10)*. Then, the gradient of the trace is given by*

$$\frac{1}{2}\nabla \mathrm{Tr}(C_\alpha) = \mathbf{1} - M\, v(\alpha) A_\alpha^{-1}\mathbf{1}, \tag{2.30}$$

where A_α is defined in (2.12)*.*

Proof. By (2.9), we have

$$\mathrm{Tr}(C_\alpha) = \mathrm{Tr}(\widetilde{C}) + 2\sum_{i=1}^{M} \alpha_i - M\, v(\alpha). \tag{2.31}$$

Combining this with (2.15) gives the gradient. □

Observe that $\mathbf{1}^T \nabla \mathrm{Tr}(C_\alpha) = 0$.

Lemma 4. *Suppose the empirical covariance matrix $\widetilde{C}$ is of full rank, and the quantities C_α, $v(\alpha)$, and A_α are as in* (2.9)*,* (2.10)*, and* (2.12) *respectively. Then, the Hessian of $\mathrm{Tr}(C_\alpha)$, denoted by $H_\alpha := \mathrm{Hess}\big(\mathrm{Tr}(C_\alpha)\big)$, is given by*

$$\frac{1}{2}H_\alpha = M\, A_\alpha^{-1} - M\, v(\alpha)\, A_\alpha^{-1}\mathbf{1}\mathbf{1}^T A_\alpha^{-1}. \tag{2.32}$$

Proof. By (2.30), (2.10), and (2.20) we have

$$\begin{aligned}
\frac{1}{2}H_\alpha &= \frac{1}{2}\nabla\left(\nabla \mathrm{Tr}(C_\alpha)\right)^T \\
&= \nabla\left[\mathbf{1}^T - M\, v(\alpha)\mathbf{1}^T A_\alpha^{-1}\right] = -M\nabla\left[v(\alpha)\mathbf{1}^T A_\alpha^{-1}\right] \\
&= -M\left[(\nabla v(\alpha))\,\mathbf{1}^T A_\alpha^{-1} + v(\alpha)\left(\nabla \mathbf{1}^T A_\alpha^{-1}\right)\right] \\
&= -M\left[2v(\alpha)A_\alpha^{-1}\mathbf{1}\mathbf{1}^T A_\alpha^{-1} + v(\alpha)\left(-A_\alpha^{-1}\mathbf{1}\mathbf{1}^T A_\alpha^{-1} - \frac{1}{v(\alpha)}A_\alpha^{-1}\right)\right] \\
&= MA_\alpha^{-1} - Mv(\alpha)A_\alpha^{-1}\mathbf{1}\mathbf{1}^T A_\alpha^{-1}. \qquad (2.33)
\end{aligned}$$

□

Theorem 2. *Suppose the empirical covariance matrix $\widetilde{C}$ is of full rank, and the quantities C_α and $v(\alpha)$ are as in* (2.9) *and* (2.10)*. Then, the trace of C_α is convex, i.e.,*

$$\triangle \mathrm{Tr}(C_\alpha) \geq 0 \quad \forall \alpha. \qquad (2.34)$$

Proof. Here, $A_\alpha = \widetilde{C} + \alpha\mathbf{1}^T + \mathbf{1}^T\alpha$ is a positive definite symmetric matrix with eigenvalues

$$\lambda_1 \geq \lambda_2 \geq \ldots \geq \lambda_M > 0.$$

Equation (2.32) implies

$$\begin{aligned}
\frac{1}{2}\triangle \mathrm{Tr}(C_\alpha) &= \frac{1}{2}\mathrm{Tr}\big(H_\alpha\big) \\
&= M\Big[\mathrm{Tr}\big(A_\alpha^{-1}\big) - v(\alpha)\mathrm{Tr}\big(A_\alpha^{-1}\mathbf{1}\mathbf{1}^T A_\alpha^{-1}\big)\Big] \\
&= M\Big[\mathrm{Tr}\big(A_\alpha^{-1}\big) - v(\alpha)\mathrm{Tr}\big(\mathbf{1}^T A_\alpha^{-2}\mathbf{1}\big)\Big] \\
&= M\Big[\mathrm{Tr}\big(A_\alpha^{-1}\big) - v(\alpha)\mathbf{1}^T A_\alpha^{-2}\mathbf{1}\Big] \\
&= M\left[\mathrm{Tr}\big(A_\alpha^{-1}\big) - \frac{\mathbf{1}^T A_\alpha^{-2}\mathbf{1}}{\mathbf{1}^T A_\alpha^{-1}\mathbf{1}}\right] \\
&\geq M\left[\mathrm{Tr}\big(A_\alpha^{-1}\big) - \frac{1}{\lambda_M}\right] \geq 0
\end{aligned} \tag{2.35}$$

as plugging $u = A_\alpha^{-1}\mathbf{1}$ into $\lambda_M \leq \frac{u^T A_\alpha u}{u^T u}$ yields $\frac{\mathbf{1}^T A_\alpha^{-2}\mathbf{1}}{\mathbf{1}^T A_\alpha^{-1}\mathbf{1}} \leq \frac{1}{\lambda_M}$. □

2.2 C-SHIFT algorithm and experiments

In this section we provide the C-SHIFT algorithm and evaluate its performance on synthetic data sets. Moreover, we compare the C-SHIFT algorithm with the well-known and frequently used normalization methods: Quantile, Rank, LOESS, and Median absolute deviation (MAD). Our empirical results demonstrate that the C-SHIFT algorithm outperforms other methods.

2.2.1 C-SHIFT algorithm

Algorithm 1 C-SHIFT

Input: observed covariance matrix $\widetilde{C}$
Output: recovered empirical covariance matrix C
if $\widetilde{C}$ is rank deficient **then**
  $f \leftarrow$ i.i.d. $\mathsf{Unif}\,[0,1]$
  $\tilde{C} \leftarrow \tilde{C} + \mathsf{diag}(f)$
end if
$v(\alpha) \leftarrow \left[\mathbf{1}^T \left(\widetilde{C} + \alpha\mathbf{1}^T + \mathbf{1}^T\alpha\right)^{-1} \mathbf{1}\right]^{-1}$
$C_\alpha \leftarrow \widetilde{C} + \alpha\mathbf{1}^T + \mathbf{1}^T\alpha - v(\alpha)\mathbf{1}\mathbf{1}^T$
$\alpha^* \leftarrow \arg\min_\alpha \|C_\alpha\|_F^2$
$C \leftarrow C_{\alpha^*}$
if $\widetilde{C}$ is rank deficient **then**
  $C \leftarrow C - \mathsf{diag}(f)$
end if
return C

The pseudocode for the C-SHIFT algorithm is given in Algorithm 1. Note that the algorithm takes into account both cases: when $\widetilde{C}$ has full rank and when $\widetilde{C}$ is rank deficient (i.e., $\widetilde{C}$ is positive semi-definite but not positive definite). When $\widetilde{C}$ is rank deficient the rank of $\widetilde{C}+\alpha\mathbf{1}^T+\mathbf{1}^T\alpha$ may exceed the rank $\widetilde{C}$ by no more than 2, and therefore may also be rank deficient. Therefore, to make $\widetilde{C}$ a full rank we add to it a diagonal matrix $\mathsf{diag}(f)$, where f is a vector of i.i.d. random variables from $\mathsf{Unif}[0,1]$.

To find the optimal $\alpha^* = \arg\min_\alpha \|C_\alpha\|_F^2$, we use the gradient and Hessian, provided in equations (2.11) and (2.16), in the trust-region algorithm to minimize $\|C_\alpha\|_F^2$.

2.2.2 Numerical experiments

In this section we conduct experiments on two synthetic datasets that we generate using random covariance method (RCM) and cascade method. We start by describing both methods.

2.2.2.1 Data generation

Random covariance method (RCM). We generate a synthetic data set with $M = 2000$ genes and $N = 50$ measurements (samples) using RCM. For that we first generate an auxiliary matrix $H \in \mathbb{R}^{M\times m}$ $(m = 2)$ whose entries are independent random variables, uniformly distributed over the interval $I = [-10, 10]$. Next, we sample a diagonal matrix $D \in \mathbb{R}^{M\times M}$ with diagonal entries being i.i.d. exponential random variables with parameter $\lambda_D = 30$. We let $\Sigma = HH^T + D$ be the population (parameter) covariance matrix. Then we generate the true empirical logarithmic data $Y^{(i)} = \big(Y_n^{(i)}\big) \sim \mathcal{N}\big(0, \Sigma\big)$ for each $i = 1, \ldots, N$. Finally, we set the observed logarithmic data be $\widetilde{Y}^{(i)} = Y^{(i)} + V^{(i)}$, where vector $V^{(i)}$ consists of M identical values drawn from $\mathcal{N}\big(-0.01, 100\big)$ random variables.

Cascade method. The *cascade* datasets were generated according by a directed acyclic weighted network $G = (V, E)$ aka directed acyclic graph (DAG). The graph was randomly generated via a recurrent *cascade* model. The parent-offspring relation is represented by the direction of edges $E = \{(u, v)\}$ of the graph G, i.e., u is the parent vertex and v is its offspring. For any vertex v let $pa(v)$ be the set

of its parents, $pa(v) = \{u \in V : (u, v) \in E\}$. Next, for each edge $(u, v) \in E$ an independent random weight c_{uv} is assigned, with c.d.f.

$$p\, U_{[a_-,b_-]}(x) + (1-p)\, U_{[a_+,b_+]}(x),$$

where the parameters $a_- < b_- \leq 0,\ 0 \leq a_+ < b_+$, and $p \in (0, 1)$ are fixed, and $U_A(x)$ denotes the uniform c.d.f. on an interval A. We generated a random weighted DAG with the nodes $v \in V$ representing the genes. The random variables $\{Y_v\}_{v \in V}$ representing the logarithmic gene expressions are generated as a noisy multiplicative cascade via the following structural linear recursive equations:

$$Y_v = \sum_{u \in pa(v)} c_{uv} Y_u + \varepsilon_v,$$

where the recursion begins with $Y_0 = y_0$, and proceeds from generation to generation. The noise variables $(\varepsilon_v, v \in V)$ are i.i.d. $\mathcal{N}\big(0, \sigma^2\big)$, sampled independently from the random weights c_{uv}. For simulation of $(Y_v, v \in V)$ the following values of parameters were chosen:

p	$[a_-, b_-]$	$[a_+, b_+]$	σ^2	y_0	$\lvert V \rvert$
1/3	$[-1.2, -0.5]$	$[0.5, 1.3]$	1	4.5	2000

2.2.2.2 Simulation results

We generate two data sets (RCM and Cascade) using the methods described in section 2.2.2.1. Each date set consists of a matrix with the empirical data

$\left(Y_n^{(i)}\right) \in \mathbb{R}^{M\times N}$ and a matrix with the observed data $\left(\widetilde{Y}_n^{(i)}\right) \in \mathbb{R}^{M\times N}$. In both, RCM and Cascade data sets, we let $M = 2000$ genes and $N = 50$ measurements (samples). For each data set, we normalize the covariance matrix $\widetilde{C}$, obtained from the observed data, by using C-SHIFT, Rank, Quantile, LOESS, and MAD methods. We compare the performance of the algorithms using the results presented in Figures 2.1-2.4.

In Figures 2.1 and 2.3 we depict the bar graphs of correlations for RCM and Cascade data sets, respectively. On the x-axis we display the range of correlations, partitioned into the intervals of length 0.1. The height of each bar represents the number of correlations that belong to the corresponding interval. Bars of different colors correspond to different correlation matrices, indicated in the legend. In particular, black and yellow bars correspond to the correlation matrices of empirical and observed data, respectively. As we can see in both data sets, the correlations of the observed data (yellow) are shifted away from -1 so that there are no large magnitude negative correlations. The aim of the normalization algorithms is to shift the correlations back into correct positions, i.e., ideally, the correlations of the normalized data should match the empirical correlations. Note that for both data sets, the C-SHIFT method correctly recovers the number of correlations in each interval: the red bars almost perfectly match the black bars. In contrast, other normalization methods could not recover the correct numbers of correlations, especially for the correlations of larger magnitudes. Specifically, Rank, Quantile and LOESS normalization techniques tend to shift correlations mostly to the center of the bar plot, each forming a bell shape. Predictably, the MAD method has

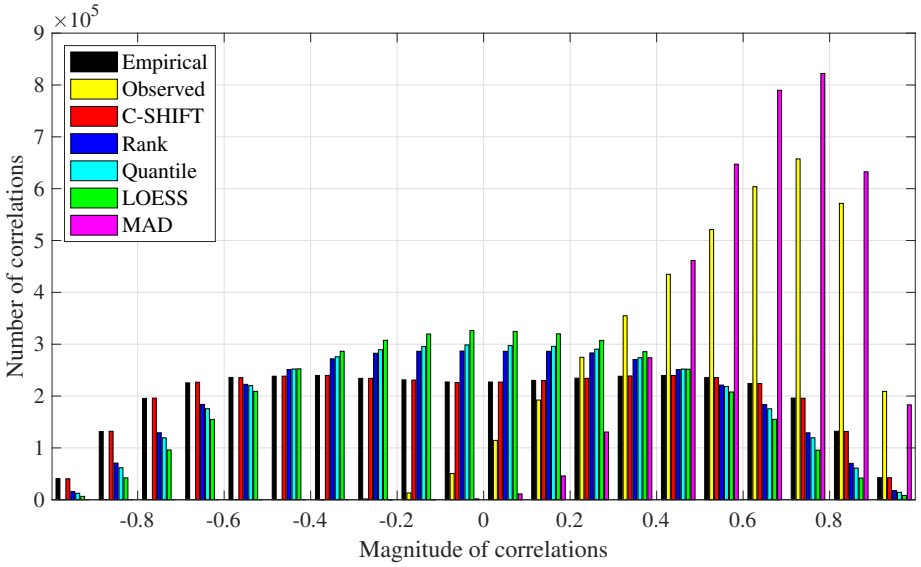

Figure 2.1: Bar graph of correlations for the RCM data set. On the x-axis we display the range of correlations, partitioned into intervals of length 0.1. The height of each bar describes the number of correlations that belong to the corresponding interval. Bars of different colors correspond to different correlation matrices, indicated in the legend.

the worst performance in correlation recovery. Finally, among the other three normalization techniques (Quantile, Rank, and LOESS), the latter method has the poorest performance.

Figures 2.2 and 2.4 contain six heat maps each, for RCM and Cascade data sets, respectively. Each heat map illustrates the transformation of the true empirical correlations $corr(Y_n, Y_m)$ (horizontal axis) after adding bias and applying the corresponding normalization method. We consider 2,001,000 correlations corresponding to all pairs of genes. For each point, representing a pair of genes (n, m), the horizontal coordinate equals the true empirical correlation $corr(Y_n, Y_m)$ in all

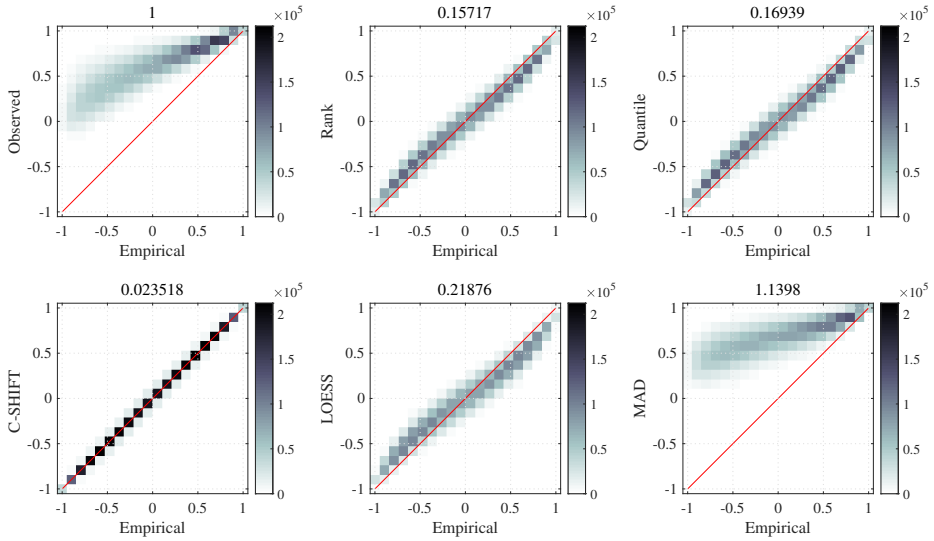

Figure 2.2: The heat maps for the RCM data set. Each heat map illustrates the transformation of the true empirical correlations $corr(Y_n, Y_m)$ (horizontal axis) after adding bias and applying the corresponding normalization method. In the top left plot the vertical axis represents the observed correlations $corr(\widetilde{Y}_n, \widetilde{Y}_m)$. In the remaining five heat maps, the vertical coordinates represent the correlations after normalization. Going clockwise, these five heat maps are Rank, Quantile, MAD, LOESS, and C-SHIFT. The darker the color, the higher the density. The number on top of each heat map indicates the relative leftover error after normalization. Smaller numbers indicate better recovery performance.

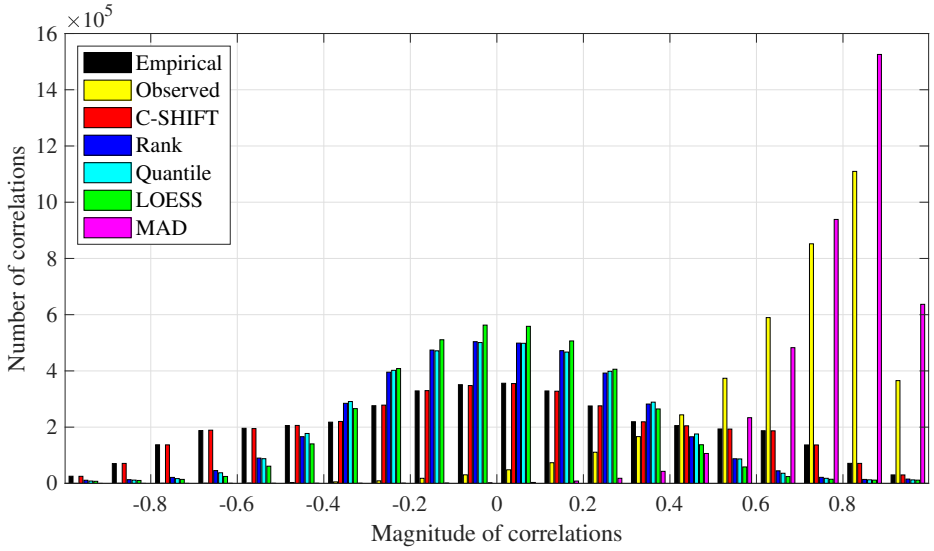

Figure 2.3: Bar graph of correlations for the Cascade data set. On the x-axis we display the range of correlations, partitioned into intervals of length 0.1. The height of each bar describes the number of correlations that belong to the corresponding interval. Bars of different colors correspond to different correlation matrices, indicated in the legend.

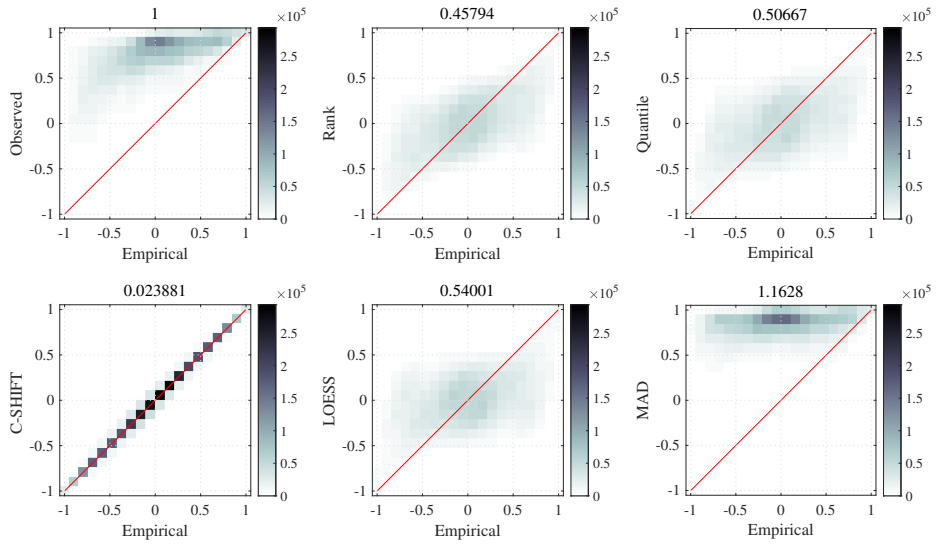

Figure 2.4: The heat maps for the Cascade data set. Each heat map illustrates the transformation of the true empirical correlations $corr(Y_n, Y_m)$ (horizontal axis) after adding bias and applying the corresponding normalization method. In the top left plot the vertical axis represents the observed correlations $corr(\widetilde{Y}_n, \widetilde{Y}_m)$. In the remaining five heat maps, the vertical coordinates represent the correlations after normalization. Going clockwise, these five heat maps are Rank, Quantile, MAD, LOESS, and C-SHIFT. The darker the color, the higher the density. The number on top of each heat map indicates the relative leftover error after normalization. Smaller numbers indicate better recovery performance.

six plots. The vertical coordinate in the top left heat map is the correlation in the observed data, $corr(\widetilde{Y}_n, \widetilde{Y}_m)$. Importantly, it shows the shift of correlations rightward in the observed data. In the remaining five heat maps, the vertical coordinates represent the correlations after normalization. Going clockwise, these five heat maps are Rank, Quantile, MAD, LOESS, and C-SHIFT. The darker the color, the higher the density. Notice that the heat map for C-SHIFT is almost perfectly diagonal, which demonstrates how well C-SHIFT recovers the correlations. Thus, in addition to correctly recovering the right numbers of correlations in each interval (which was demonstrated in Figures 2.1 and 2.3), the proposed C-SHIFT algorithm also returns (shifts back) the correlations to the correct margins. Hence, the heat map is a diagonal line. The number on top of each heat map indicates the relative leftover error after normalization, i.e., the ℓ^2-norm of the vector of differences between the horizontal and vertical coordinates, scaled by the Frobenius norm of the difference between the empirical and the observed correlation matrices. Thus, the left top heat map is assigned the value 1, and for each normalization method, the smaller the number the better it recovers the empirical correlation matrix. Any such number smaller than one is an improvement. The number for C-SHIFT is by far the smallest in each data set (0.023518 and 0.023881), while in the case of MAD normalization, the corresponding number even exceeds 1.

2.3 Discussion

In systems biology, the gene co-expression networks (GCN) are reconstructed from the correlations between the genes. GCN recovery relies on removing the bias with a normalization method, and thus improving the estimation of correlations between the pairs of genes. However, the standard normalization techniques are known to be insufficient at recovering the true empirical correlations while the C-SHIFT algorithm is specifically designed to recover the true empirical correlations. The multiple experiments with synthetic data sets demonstrate the algorithm's superior performance in comparison to the standard normalization techniques.

Finally, notice that the C-SHIFT algorithm corrects the positive shift of covariances (and correlations) observed when $\hat{\omega} = \widehat{Var}(V)$ is larger than $\hat{a}_n = -\widehat{Cov}(Y_n, V)$ $(n = 1, \ldots, M)$ in (2.7). Hence, the independence of V from Y_n assumption can be replaced with $Cov(Y_n, V) \ll Var(V)$.

The bulk of the work in this chapter has been submitted for publication [10].

2.4 Effect on t-test

The C-SHIFT algorithm focuses on reclaiming the underlying correlation structure directly without altering the observed data. However, every other normalizing method does alter the data itself. While they all do a poor job of recapturing the correlation structure inherent in the system, they have generally been used for another reason. Before the network structure is analyzed (via correlation structure), two sample t-tests are generally done between two clinical groups (e.g., healthy

and sick/diseased) to determine which genes are even important to the condition being studied. The various normalization techniques were created to address the effect of the technical noise on these tests.

Therefore, we wished to investigate the performance of the different normalization methods on the process of testing each gene for differential expression between the two groups. A simulation study was performed for this reason. The goal was to calculate the average number of true and false positives across 1000 simulations for each set of conditions. The simulated data came from a system with 200 genes (50 of which were differentially expressed) and 50 samples (25 in each group). The conditions are defined by three factors. The first factor is the size of the differential expressions, which were either small (sampled from Uniform(2, 6)) or large (sampled from Uniform(9, 15)). The second factor is the size of the noise (log W), which was either small (sampled from $N(0, 2^2)$) or large (sampled from $N(0, 10^2)$). The third factor was whether the differential expression was on average half positive/half negative (both) or all positive. The underlying covariance structure was generated using RCM ($m = 2$) as in section 2.2.2.1. The results while averaging over the third factor (only positive DE or both) are shown in figure 2.5 and table 2.1.

With small (and more realistic) noise, Quantile normalization has notably fewer false positives than when directly using the observed data. If the size of the differential expression between groups is small, Quantile does lose power. However, with much smaller false discovery rates (and very large total number of genes/tests), it is generally a good trade off. For larger noise, the benefits of Quantile normalization

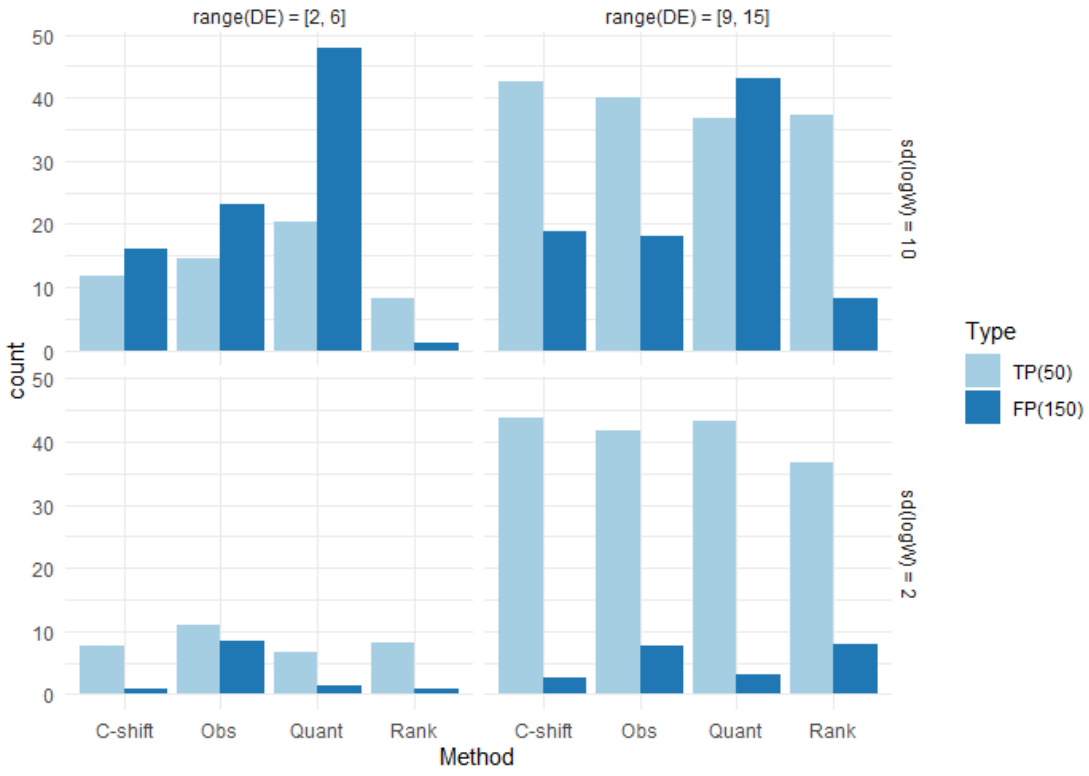

Figure 2.5: Bar graphs showing the average number of true positives (out of 50) and false positives (out of 150) on the y-axis. The x-axis denotes the normalization method (or lack there of, i.e., "Obs" denotes no normalization method used). The left (right) column in the grid of bar graphs corresponds to a small (large) amount of differential expression. The top (bottom) row of graphs corresponds to a large (small) amount of sample level additive noise to the logged data. Bars of different colors correspond to true (light blue) and false (dark blue) positives as indicated in the legend.

over the observed data disappear as the false discovery rates become unacceptable.

For small noise, the tests performed with variances corrected by the C-SHIFT algorithm produced improvements overall using directly observed data similar to the improvements of Quantile. However, the C-SHIFT results were even better (more true and less false discoveries) than Quantile. With large noise, the corrected variances decrease the number of both the true and the false discoveries compared to the observed data if the magnitude of the differential expression between groups is small. In the case of larger sized differential expression, the C-SHIFT results are similar to the observed data, but with a small increase in the number of true discoveries.

Rank normalization does just as well as C-SHIFT (better than Quantile and observed) when both the noise and size of differential expression is small. When the noise is small, but the differential expression is large, rank performs worse than the alternatives. It arguably performs the best when there is large noise, however, this is dependent on the distribution of the differential expression. Specifically, performance is high when the number of positively and negatively deferentially expressed genes is fairly equal, but gets worse under any imbalance as seen in figure 2.6.

In table 2.1, we can see that in any scenario that the calculated False Discovery Proportions (FDP) are lower or similar when using C-SHIFT corrected variances than with observed variances. Quantile normalized data produces improved FDPs when there is small noise, but worse FDPs when there is large noise. Rank normalization produces lower FDPs when there is a fairly even number of positive

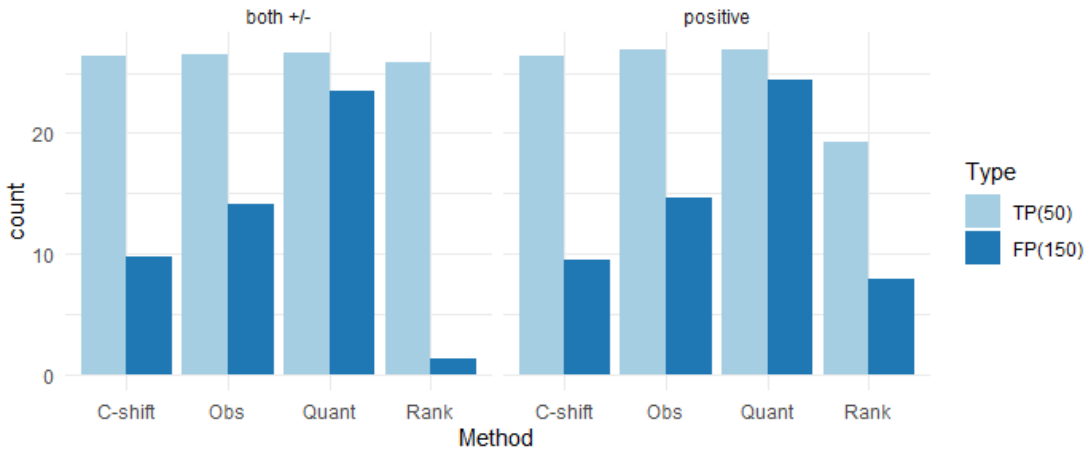

Figure 2.6: Bar graphs show the average number of true positives (out of 50) and false positives (out of 150) on the y-axis. The x-axis denotes the normalization method (or lack there of, i.e., "Obs" denotes no normalization method used). The left (right) column in the grid of bar graphs corresponds to when the number of positively and negatively deferentially expressed genes is fairly equal (only positive differential expression). Bars of different colors correspond to true (light blue) and false (dark blue) positives as shown in the legend.

and negative differential expression, but has mixed results when all differential expression is positive.

Table 2.1: Calculated False Discovery Proportions (FDP) for each set of simulations done with observed data and data normalized with C-SHIFT, quantile, and rank normalization methods.

				FDP			
	DE balance	sd(logW)	range(DE)	C-shift	Obs	Quant	Rank
1	both +/-	2	[2, 6]	0.093	0.434	0.202	0.044
2	both +/-	2	[9, 15]	0.060	0.156	0.075	0.046
3	both +/-	10	[2, 6]	0.585	0.620	0.707	0.060
4	both +/-	10	[9, 15]	0.305	0.303	0.534	0.044
5	positive	2	[2, 6]	0.091	0.441	0.167	0.191
6	positive	2	[9, 15]	0.057	0.155	0.064	0.299
7	positive	10	[2, 6]	0.568	0.613	0.697	0.208
8	positive	10	[9, 15]	0.307	0.321	0.545	0.310

3 How quantile normalization may improve the t-test in a noiseless environment

3.1 Background

In the previous chapter we found that while C-SHIFT normalization generally produced the best false discovery rates, quantile normalization also showed improvement over the raw observed data in this regard. In this chapter we explore the possibility that quantile normalization might improve the power of Welch's t-test even when data is not biased as it was in the previous chapter. A simple simulation study was done using data generated in the exact same way as described in 2.4. The settings used correspond to the large magnitude differential expressions that are balanced in sign, but with 10,000 simulations. Performing the tests with the observed data yielded a false discovery proportion of 0.166, while the tests done on the quantile normalized data resulted in an FDP of 0.073. This difference is the culmination of both more true positives and less false negatives using quantile normalization. It is the first effect that we focus on in this chapter.

Suppose $Z = \begin{pmatrix} Z_1 \\ Z_2 \\ \vdots \\ Z_N \end{pmatrix}$ is a continuously distributed random vector with mean

$$\mu = \mathrm{E}[Z] = \begin{pmatrix} \mu_1 \\ \mu_2 \\ \vdots \\ \mu_N \end{pmatrix}$$

and covariance matrix Σ. Let $X = \begin{pmatrix} X_1 \\ X_2 \\ \vdots \\ X_N \end{pmatrix}$ be the rank order statistic of margins in Z. Next, for any gene j, we define a Bernoulli random vector B_j as follows

$$B_j = \vec{e}_k \quad \text{with probability } p_{j,k} = P(Z_j = X_k).$$

Then,

$$Z_j = B_j \cdot X,$$

where B_j and X are dependent random vectors unless $Z_1, \ldots, Z_N$ are exchangeable.

Importantly, observe that

$$\mathcal{P} = \Big(p_{j,k}\Big)_{j,k=1,\ldots,N}$$

is a **doubly stochastic matrix**. Thus, $\mathcal{P}^*\mathcal{P}$ is a symmetric and doubly stochastic matrix. Letting $\mathcal{B} = \begin{pmatrix} - & B_1^* & - \\ \vdots & \vdots & \vdots \\ - & B_m^* & - \end{pmatrix}$, be the matrix with rows B_j^*, we have $\mathrm{E}[\mathcal{B}] = \mathcal{P}$. Finally, denote $\pi_j = \mathrm{E}[B_j] = \begin{pmatrix} p_{j,1} \\ \vdots \\ p_{j,N} \end{pmatrix} = \mathcal{P}^* e_j$, and $\mu_{\mathrm{x}} = \mathrm{E}[X]$.

Given a gene j. The estimation done for m samples produces the sample average equal to

$$\overline{Z_j} = \overline{B_j \cdot X} = \frac{1}{m} \sum_{k=1}^{m} B_j^{(k)} \cdot X^{(k)}.$$

Given a gene j. The estimation done **after quantile normalization** for m samples produces the sample average equal to

$$\overline{Q_j} = \overline{B_j} \cdot \overline{X} = \frac{1}{m} \sum_{k=1}^{m} B_j^{(k)} \cdot \frac{1}{m} \sum_{i=1}^{m} X^{(i)} = \frac{1}{m^2} \sum_{i,k=1}^{m} B_j^{(k)} \cdot X^{(i)}.$$

Then

$$\mathrm{E}[\overline{Q_j}] = \left(1 - \frac{1}{m}\right) \pi_j^* \mu_{\mathrm{x}} + \frac{1}{m} \mu_j,$$

where $\mu_j = \mathrm{E}[Z_j]$. Since $\sum_{j=1}^{N} \pi_j = \mathcal{P}^*\mathbf{1} = \mathbf{1}$,

$$\begin{aligned}\sum_{j=1}^{N} \mathrm{E}[\overline{Q_j}] &= \left(1 - \frac{1}{m}\right) \mathrm{E}[\mathbf{1} \cdot X] + \frac{1}{m} \sum_{j=1}^{N} \mu_j \\ &= \left(1 - \frac{1}{m}\right) \mathrm{E}[\mathbf{1} \cdot Z] + \frac{1}{m} \sum_{j=1}^{N} \mu_j = \sum_{j=1}^{N} \mathrm{E}[\overline{Z_j}].\end{aligned}$$

Let $\overline{Q}$ and $\overline{Z}$ denote the vectors with coordinates $\overline{Q_j}$ and $\overline{Z_j}$ respectively. Then, we have shown that

$$\mathrm{E}[\mathbf{1}^*\overline{Q}] = \mathrm{E}[\mathbf{1}^*\overline{Z}].$$

Throughout this chapter we will define the variance and covariance for random vectors as follows,

$$\mathrm{Var}(\xi) = \mathrm{E}\left[\xi^T\xi\right] - \mathrm{E}\left[\xi\right]^T \mathrm{E}\left[\xi\right] \quad \text{and} \quad \mathrm{Cov}(\xi_1, \xi_2) = \mathrm{E}\left[\xi_1^T\xi_2\right] - \mathrm{E}\left[\xi_1\right]^T \mathrm{E}\left[\xi_2\right].$$

3.2 Theory and results

The following assumption is easy to validate for most practical continuous distributions of Z.

Assumption **1.** Assume that the symmetric and doubly stochastic matrix $\mathcal{P}^*\mathcal{P}$ is irreducible and aperiodic.

Observe that if the above Assumption 1 is satisfied, then, by the Perron-Frobenius theorem, $\lambda_1 = 1$ is the largest eigenvalue of $\mathcal{P}^*\mathcal{P}$. Furthermore, λ_1 has algebraic

and geometric multiplicity one, and $\mathbf{1}$ is the corresponding eigenvector. In this case, we let

$$1 > \lambda_2 \geq \ldots \geq \lambda_N \geq 0$$

denote all other eigenvalues of matrix $\mathcal{P}^*\mathcal{P}$ starting from the second largest λ_2 and ending with the smallest eigenvalue λ_N.

Our next assumption was validated for the two dimensional normal distributions in Section 3.4. Let $\Pi = \frac{1}{N}\mathbf{1}\mathbf{1}^*$ be the orthogonal projection on the normal line

$$x_1 = x_2 = \ldots = x_N.$$

Assumption **2.** Assume that the quantity

$$\delta_0 := \left\| \frac{E\big[(I-\Pi)Z\big]}{\sqrt{\mathrm{Var}\left((I-\Pi)Z\right)}} \right\|_2^2 \tag{3.1}$$

is suitably small.

Note that $(I-\Pi)$ is the orthogonal projection onto hyperspace $\mathbf{1}x = 0$, and $(I-\Pi)^2 = (I-\Pi)$. Assumption 2 is equivalent to the positive quantity

$$\delta := \frac{\delta_0}{1+\delta_0} = \frac{\mu^*(I-\Pi)\mu}{E\big[Z^*(I-\Pi)Z\big]} = \frac{\big\|E\big[(I-\Pi)Z\big]\big\|_2^2}{E\big[\|(I-\Pi)Z\|_2^2\big]} \tag{3.2}$$

being suitably small.

Next, notice that

$$E\big[(Z-\mu)^*\Pi(Z-\mu)\big] = \mathrm{Tr}(\Pi\Sigma)$$

and therefore we have

$$E\big[\|\Pi Z\|_2^2\big] = \mu^*\Pi\mu + \mathrm{Tr}(\Pi\Sigma) \tag{3.3}$$

and

$$\begin{aligned} E\big[Z^*(I-\Pi)Z\big] &= E\big[(Z-\mu)^*(I-\Pi)(Z-\mu)\big] + \mu^*(I-\Pi)\mu \\ &= \mathrm{Tr}(\Sigma) - \mathrm{Tr}(\Pi\Sigma) + \mu^*(I-\Pi)\mu. \end{aligned} \tag{3.4}$$

We use equation (3.4) to rewrite (3.2) as follows:

$$\frac{1}{\delta_0}\mu^*(I-\Pi)\mu = \mathrm{Tr}(\Sigma) - \mathrm{Tr}(\Pi\Sigma). \tag{3.5}$$

Assumption **3.** Assume that $\mathrm{Tr}(\Pi\Sigma) > 0$.

Observe that since the $\mathrm{Tr}(\Pi\Sigma) = \frac{1}{N}\mathbf{1}^*\Sigma\mathbf{1} \geq 0$, the only exception to Assumption 3 is the case when the $\mathrm{Tr}(\Pi\Sigma) = 0$. This type of exception may occur when the dependence of $Z_1, \ldots, Z_N$ is based on conditioning upon

$$Z_1 + \ldots + Z_N = C_0$$

for a given constant C_0, e.g. when the random variables $Z_1, \ldots, Z_N$ are the incre-

ments of a Brownian Bridge.

Under Assumption 3, we define the quantity

$$\delta'' = \frac{\mathrm{Tr}(\Sigma)}{\mathrm{Tr}(\Pi\Sigma)} - 1 \ \geq 0. \tag{3.6}$$

Notice that $\mathrm{Tr}(\Sigma) = \mathrm{Var}(Z)$, and that $\mathrm{Tr}(AB) = \mathrm{Tr}(BA)$ implies

$$\mathrm{Var}(\Pi Z) = \frac{1}{N}\mathbf{1}^*\Sigma\mathbf{1} = \mathrm{Tr}(\Pi\Sigma).$$

Hence, the above equation (3.6) is equivalent to

$$(1+\delta'')\,\mathrm{Var}(\Pi Z) = \mathrm{Var}(Z). \tag{3.7}$$

Theorem 3. *Under the assumptions 1-3 with sufficiently small δ and suitable parameters λ_2, λ_N, and δ'',*

$$\mathrm{Var}(\overline{Q}) < \mathrm{Var}(\overline{Z}).$$

Corollary 1. *Consider two populations A and B of respective sizes N_A and N_B. Under the assumptions 1-3 with suitable parameters, we have*

$$\frac{\left|\mathrm{E}[\mathbf{1}^*\overline{Q}_A] - \mathrm{E}[\mathbf{1}^*\overline{Q}_B]\right|}{\left(\frac{N_A}{N_A+N_B}\,\mathrm{Var}(\overline{Q}_A) + \frac{N_B}{N_A+N_B}\,\mathrm{Var}(\overline{Q}_B)\right)^{1/2}} > \frac{\left|\mathrm{E}[\mathbf{1}^*\overline{Z}_A] - \mathrm{E}[\mathbf{1}^*\overline{Z}_B]\right|}{\left(\frac{N_A}{N_A+N_B}\,\mathrm{Var}(\overline{Z}_A) + \frac{N_B}{N_A+N_B}\,\mathrm{Var}(\overline{Z}_B)\right)^{1/2}}.$$

3.3 Supplementary results and proofs

Lemma 5.

$$\mathrm{Var}(\overline{Q_j}) = \frac{1}{m}\Big(\pi_j^*\Sigma_{\mathsf{x}}\pi_j + \mu_{\mathsf{x}}^*\Sigma_{B_j}\mu_{\mathsf{x}} + 2\ \mathrm{Cov}(\mu_{\mathsf{x}}^*B_j, \pi_j^*X)\Big) + \mathcal{E}_j, \tag{3.8}$$

where $\mu_{\mathsf{x}} = \mathrm{E}[X]$, Σ_{x} *is the covariance matrix for* X, *and*

$$\Sigma_{B_j} = \mathcal{D}_j - \pi_j\pi_j^*, \qquad \mathcal{D}_j = \begin{pmatrix} p_{j,1} & 0 & \dots & 0 \\ 0 & p_{j,2} & \ddots & \vdots \\ \vdots & \ddots & \ddots & \vdots \\ 0 & 0 & \dots & p_{j,N} \end{pmatrix},$$

is the covariance matrix for B_j. *The error term is expressed as*

$$\begin{aligned}\mathcal{E}_j =& \frac{m-1}{m^3}\,\mathrm{Cov}\left(Z_j,\ \pi_j^*X\right) + \frac{m-1}{m^3}\,\mathrm{Cov}\left(Z_j,\ \mu_{\mathsf{x}}^*B_j\right) + \frac{1}{m^3}\,\mathrm{Var}(Z_j) \\ &- \frac{3m-2}{m^3}\left(\pi_j^*\Sigma_{\mathsf{x}}\pi_j + \mu_{\mathsf{x}}^*\Sigma_{B_j}\mu_{\mathsf{x}} + 2\ \mathrm{Cov}(\mu_{\mathsf{x}}^*B_j, \pi_j^*X)\right) \\ &+ \frac{m-1}{m^3}\left(\mathrm{E}[X^*B_jB_j^*X] - \left(\pi_j\cdot\mu_{\mathsf{x}}\right)^2\right).\end{aligned} \tag{3.9}$$

Proof. For each ${}^mP_3 = m!/(m-3)!$ non-matching triplet (k_1, k_2, i) in $\{1, 2, \dots, m\}$,

$$\begin{aligned}\mathrm{Cov}\left(B_j^{(k_1)}\cdot X^{(i)}, B_j^{(k_2)}\cdot X^{(i)}\right) &= \pi_j^*E\left[\left(X^{(i)}-\mu_{\mathsf{x}}\right)\left(X^{(i)}-\mu_{\mathsf{x}}\right)^*\right]\pi_j \\ &= \pi_j^*\Sigma_{\mathsf{x}}\pi_j.\end{aligned}$$

Similarly, for each ${}^mP_3$ non-matching triplet (k_1, k_2, i) in $\{1, 2, \ldots, m\}$,

$$\begin{aligned}\mathrm{Cov}\left(B_j^{(k)} \cdot X^{(i_1)}, B_j^{(k)} \cdot X^{(i_2)}\right) &= \mu_{\mathsf{x}}^* E\left[\left(B_j^{(k)} - \pi_j\right)\left(B_j^{(k)} - \pi_j\right)^*\right] \mu_{\mathsf{x}} \\ &= \mu_{\mathsf{x}}^* \Sigma_{B_j} \mu_{\mathsf{x}}.\end{aligned}$$

Also, for each ${}^mP_3$ non-matching triplet (k_1, k_2, i) in $\{1, 2, \ldots, m\}$,

$$\mathrm{Cov}\left(B_j^{(k)} \cdot X^{(i_1)}, B_j^{(i_2)} \cdot X^{(k)}\right) = \mu_{\mathsf{x}}^* \,\mathrm{Cov}(B_j, X)\pi_j = \mu_{\mathsf{x}}^* E\left[B_j X^*\right] \pi_j - \left(\pi_j \cdot \mu_{\mathsf{x}}\right)^2.$$

Finally, for each ${}^mP_2 = m!/(m-2)!$ non-matching doublet $k \neq i$,

$$\mathrm{Cov}\left(B_j^{(k)} \cdot X^{(i)}, B_j^{(i)} \cdot X^{(i)}\right) = E\left[(Z_j - \mu_j)\pi_j^*\big(X - \mu_{\mathsf{x}}\big)\right] = \mathrm{Cov}\left(Z_j,\, \pi_j^* X\right),$$

$$\mathrm{Cov}\left(B_j^{(k)} \cdot X^{(i)}, B_j^{(k)} \cdot X^{(k)}\right) = E\left[(Z_j - \mu_j)\mu_{\mathsf{x}}^*\big(B_j - \pi_j\big)\right] = \mathrm{Cov}\left(Z_j,\, \mu_{\mathsf{x}}^* B_j\right),$$

and

$$\mathrm{Var}\left(B_j^{(k)} \cdot X^{(i)}\right) = \mathrm{E}[X^* B_j B_j^* X] - \left(\pi_j \cdot \mu_{\mathsf{x}}\right)^2.$$

Therefore, the statement of the lemma follows as $\frac{m(m-1)(m-2)}{m^4} = \frac{1}{m} - \frac{3m-2}{m^3}$. □

Lemma 6.

$$\begin{aligned}
&\mathrm{Var}(\overline{Q}) \\
&=\frac{1}{m}\left(\mathrm{Var}(Z)+\mu^*\mu-\mathrm{Var}(X)+\mathrm{Var}(\mathcal{P}X)-\|\mathcal{P}\mu_{\mathsf{x}}\|_2^2+2\ \mathrm{Cov}\left(\mathcal{B}\mu_{\mathsf{x}},\ \mathcal{P}X\right)\right) \\
&\quad+\frac{m-1}{m^3}\left(\mathrm{Cov}\left(Z,\ \mathcal{P}X\right)+\mu_{\mathsf{x}}^*\mu_{\mathsf{x}}-\mu^*\mathcal{P}\mu_{\mathsf{x}}\right)-\frac{2m-1}{m^3}\left(\mu^*\mu-\|\mathcal{P}\mu_{\mathsf{x}}\|_2^2\right) \\
&\quad-\frac{3m-2}{m^3}\left(2\ \mathrm{Cov}\left(\mathcal{B}\mu_{\mathsf{x}},\ \mathcal{P}X\right)-\mathrm{Var}(X)+\mathrm{Var}(\mathcal{P}X)\right)-2\frac{m-1}{m^3}\mathrm{Var}(Z)
\end{aligned} \tag{3.10}$$

Proof. Since $\mathrm{Var}(\overline{Q})=\sum_{j=1}^{N}\mathrm{Var}(\overline{Q_j})$, we sum over j for the different parts of equations (3.8) and (3.9). First, observe that

$$\begin{aligned}
\pi_j^*\Sigma_{\mathsf{x}}\pi_j+\mu_{\mathsf{x}}^*\Sigma_{B_j}\mu_{\mathsf{x}} &= \pi_j^*\left(\mathrm{E}[XX^*]-\mu_{\mathsf{x}}\mu_{\mathsf{x}}^*\right)\pi_j+\mu_{\mathsf{x}}^*\left(\mathcal{D}_j-\pi_j\pi_j^*\right)\mu_{\mathsf{x}} \\
&= \mathrm{Var}(\pi_j\cdot X)+\mu_{\mathsf{x}}^*\mathcal{D}_j\mu_{\mathsf{x}}-\left(\pi_j\cdot\mu_{\mathsf{x}}\right)^2,
\end{aligned} \tag{3.11}$$

where $\sum_{j=1}^{N}p_{j,k}=1$ (for all $k=1,\ldots,N$) implies $\sum_{j=1}^{N}\mu_{\mathsf{x}}^*\mathcal{D}_j\mu_{\mathsf{x}}=\mu_{\mathsf{x}}^*\mu_{\mathsf{x}}$. Thus, by

(3.11),

$$\begin{aligned}\sum_{j=1}^{N}\left(\pi_j^*\Sigma_{\mathsf{x}}\pi_j+\mu_{\mathsf{x}}^*\Sigma_{B_j}\mu_{\mathsf{x}}\right) &= \mu_{\mathsf{x}}^*\mu_{\mathsf{x}}+\sum_{j=1}^{N}\mathrm{Var}(\pi_j\cdot X)-\sum_{j=1}^{N}\left(\pi_j\cdot\mu_{\mathsf{x}}\right)^2\\ &= E\big[X^*X\big]-\mathrm{Var}(X)+\mathrm{Var}(\mathcal{P}X)-\|\mathcal{P}\mu_{\mathsf{x}}\|_2^2\\ &= E\big[Z^*Z\big]-\mathrm{Var}(X)+\mathrm{Var}(\mathcal{P}X)-\|\mathcal{P}\mu_{\mathsf{x}}\|_2^2\\ &= \mathrm{Var}(Z)+\mu^*\mu-\mathrm{Var}(X)+\mathrm{Var}(\mathcal{P}X)-\|\mathcal{P}\mu_{\mathsf{x}}\|_2^2.\end{aligned} \tag{3.12}$$

Also,

$$\begin{aligned}\sum_{j=1}^{N}\mathrm{Cov}(\mu_{\mathsf{x}}^*B_j,\pi_j^*X) &= \mu_{\mathsf{x}}E\left[\left(\sum_{j=1}^{N}B_je_j^*\right)\mathcal{P}X\right]-\|\mathcal{P}\mu_{\mathsf{x}}\|_2^2\\ &= \mu_{\mathsf{x}}\,\mathrm{E}[\mathcal{B}^*\mathcal{P}X]-\|\mathcal{P}\mu_{\mathsf{x}}\|_2^2=\mathrm{Cov}\left(\mathcal{B}\mu_{\mathsf{x}},\ \mathcal{P}X\right).\end{aligned} \tag{3.13}$$

Equations (3.12) and (3.13) imply

$$\begin{aligned}&\mathrm{Var}(Z)-\sum_{j=1}^{N}\left(\pi_j^*\Sigma_{\mathsf{x}}\pi_j+\mu_{\mathsf{x}}^*\Sigma_{B_j}\mu_{\mathsf{x}}+2\ \mathrm{Cov}(\mu_{\mathsf{x}}^*B_j,\pi_j^*X)\right)\\ &\qquad=\mathrm{Var}(X)-\mathrm{Var}(\mathcal{P}X)+\|\mathcal{P}\mu_{\mathsf{x}}\|_2^2-2\ \mathrm{Cov}\left(\mathcal{B}\mu_{\mathsf{x}},\ \mathcal{P}X\right)-\mu^*\mu.\end{aligned} \tag{3.14}$$

The sums that do not contribute to the $1/m$ term are

$$\begin{aligned}\sum_{j=1}^{N} \operatorname{Cov}\left(Z_j, \pi_j^* X\right) &= \sum_{j=1}^{N} \operatorname{E}\left[(Z_j - \mu_j)\pi_j^*(X - \mu_{\mathsf{x}})\right] \\ &= \sum_{j=1}^{N} \operatorname{E}\left[(Z_j - \mu_j)e_j^*\mathcal{P}(X - \mu_{\mathsf{x}})\right] \\ &= \operatorname{E}\left[(Z - \mu)^*\mathcal{P}(X - \mu_{\mathsf{x}})\right] = \operatorname{Cov}\left(Z,\ \mathcal{P}X\right),\end{aligned}$$

$$\begin{aligned}\sum_{j=1}^{N} \operatorname{Cov}(Z_j, \mu_{\mathsf{x}}^*\mathcal{B}) &= \sum_{j=1}^{N} \operatorname{E}\left[(Z_j - \mu_j)(B_j - \pi_j)^*\mu_{\mathsf{x}}\right] \\ &= \sum_{j=1}^{N} \operatorname{E}\left[(Z_j - \mu_j)(B_j^* - e_j^*\mathcal{P})\mu_{\mathsf{x}}\right] \\ &= \left(\operatorname{E}\left[X^*\left(\sum_{j=1}^{N} B_j B_j^*\right)\right] - \sum_{j=1}^{N} \mu_j \operatorname{E}\left[B_j^*\right] - \operatorname{E}\left[Z^*\right]\mathcal{P} + \mu^*\mathcal{P}\right)\mu_{\mathsf{x}} \\ &= \mu_{\mathsf{x}}^*\mu_{\mathsf{x}} - \mu^*\mathcal{P}\mu_{\mathsf{x}},\end{aligned}$$

$$\begin{aligned}\sum_{j=1}^{N} \operatorname{E}\left[X^* B_j B_j^* X\right] &= \operatorname{E}\left[X^*\left(\sum_{j=1}^{N} B_j B_j^*\right) X\right] = \operatorname{E}\left[X^* X\right] = \operatorname{E}\left[Z^* Z\right] \\ &= \operatorname{Var}(Z) + \mu^*\mu,\end{aligned}$$

and

$$\sum_{j=1}^{N} \left(\pi_j \cdot \mu_{\mathsf{x}}\right)^2 = \mu_{\mathsf{x}}^*\left(\sum_{j=1}^{N} \pi_j \pi_j^*\right)\mu_{\mathsf{x}} = \mu_{\mathsf{x}}^*\mathcal{P}\mathcal{P}^*\mu_{\mathsf{x}}.$$

Combining the various summed terms with the matching coefficients gives (3.10).

□

Lemma 7.

$$\mathrm{Var}(\overline{Z}) - \mathrm{Var}(\overline{Q}) = \frac{1}{m}M + \mathcal{E} \tag{3.15}$$

where

$$M := \ \mathrm{Var}(X) - \mathrm{Var}(\mathcal{P}X) - \mu^*\mu + \|\mathcal{P}\mu_{\mathsf{x}}\|_2^2 - 2\ \mathrm{Cov}\left(\mathcal{B}\mu_{\mathsf{x}},\ \mathcal{P}X\right) \tag{3.16}$$

and

$$\begin{aligned}\mathcal{E} = {} & 2\frac{m-1}{m^3}\,\mathrm{Var}(Z) + \frac{3m-2}{m^3}\left(2\ \mathrm{Cov}\left(\mathcal{B}\mu_{\mathsf{x}},\ \mathcal{P}X\right) - \mathrm{Var}(X) + \mathrm{Var}(\mathcal{P}X)\right) \\ & - \frac{m-1}{m^3}\left(\mathrm{Cov}\left(Z,\ \mathcal{P}X\right) + \mu_{\mathsf{x}}^*\mu_{\mathsf{x}} - \mu^*\mathcal{P}\mu_{\mathsf{x}}\right) + \frac{2m-1}{m^3}\left(\mu^*\mu - \|\mathcal{P}\mu_{\mathsf{x}}\|_2^2\right)\end{aligned} \tag{3.17}$$

is $\mathcal{O}(1/m^2)$.

Proof. Recall that $\mathrm{Var}(\overline{Z}) = \frac{1}{m}\,\mathrm{Var}(Z)$. Thus,

$$\mathrm{Var}(\overline{Z}) - \mathrm{Var}(\overline{Q}) = \frac{1}{m}\,\mathrm{Var}(Z) - \mathrm{Var}(\overline{Q}).$$

Therefore, the statement of the lemma follows by plugging in equation (3.10) and grouping terms by simplified common coefficients.

□

Lemma 8.

$$\mathrm{Var}(Z) \geq \mathrm{Var}(X)$$

Proof. First, observe that $E\big[X^*X\big] = E\big[Z^*Z\big]$. Next, Karamata's inequality implies

$$\mu_{\mathsf{x}}^*\mu_{\mathsf{x}} \geq \mu^*\mu$$

as the sequence $e_j^*\mu_{\mathsf{x}} = \mathrm{E}[X_j]$ majorizes sequence $\mu_j = \mathrm{E}[Z_j]$. Hence,

$$\mathrm{Var}(Z) = E\big[Z^*Z\big] - \mu^*\mu \geq \mathrm{Var}(X) = E\big[X^*X\big] - \mu_{\mathsf{x}}^*\mu_{\mathsf{x}}$$

□

Lemma 9.

$$\mathrm{Var}(X) \geq \mathrm{Var}(\mathcal{P}X)$$

Proof.

$$\mathrm{Var}(X) - \mathrm{Var}(\mathcal{P}X) = E\left[(X-\mu_{\mathsf{x}})^*\big(I-\mathcal{P}^*\mathcal{P}\big)(X-\mu_{\mathsf{x}})\right],$$

where $I-\mathcal{P}^*\mathcal{P}$ is symmetric with all real eigenvalues. Finally, since $\mathcal{P}^*\mathcal{P}$ is doubly stochastic, $I-\mathcal{P}^*\mathcal{P}$ is non-negative definite by Gershgorin circle theorem.

We conclude that

$$E\left[(X-\mu_{\mathsf{x}})^*\big(I-\mathcal{P}^*\mathcal{P}\big)(X-\mu_{\mathsf{x}})\right] \geq 0.$$

□

Lemma 10. *The matrix* $\mathcal{P}^*\mathcal{P} - \Pi$ *is positive definite. Also, let* $0 \leq \lambda_2 \leq 1$ *denote the second largest eigenvalue of* $\mathcal{P}^*\mathcal{P}$*, then*

$$\|\mathcal{P}^*\mathcal{P} - \Pi\|_2 = \lambda_2. \tag{3.18}$$

Note that $\lambda_2 = 1$ unless Assumption 1 is conditioned upon.

Proof. By Jensen's (or Karamata's) inequality, for all $y \in \mathbb{R}^N$,

$$\|y\|_2^2 \geq \|\Pi y\|_2^2.$$

Thus, for all $x \in \mathbb{R}^N$,

$$x^*\mathcal{P}^*\mathcal{P}x = \|\mathcal{P}x\|_2^2 \geq \|\Pi\mathcal{P}x\|_2^2 = \|\Pi x\|_2^2 = x^*\Pi^*\Pi x$$

as $\Pi\mathcal{P} = \Pi$ by double-stochasticity of $\mathcal{P}$.

Finally, the equation (3.18) follows from Π being the projection matrix on an eigenvector $\mathbf{1}$ corresponding to the largest eigenvalue $\lambda_1 = 1$ of $\mathcal{P}^*\mathcal{P}$. □

Lemma 11. *Under assumption 1,*

$$\sqrt{\lambda_N}\|(I - \Pi)x\|_2 \leq \|(\mathcal{P} - \Pi)x\|_2 \leq \sqrt{\lambda_2}\|(I - \Pi)x\|_2 \qquad \forall x \in \mathbb{R}^N,$$

where $0 \leq \lambda_N < 1$ *denotes the smallest eigenvalue of* $\mathcal{P}^*\mathcal{P}$*, and once again,* $0 \leq \lambda_2 < 1$ *denotes the second largest eigenvalue of* $\mathcal{P}^*\mathcal{P}$*.*

Proof.

$$\|(\mathcal{P}-\Pi)x\|_2^2 = \|\mathcal{P}(I-\Pi)x\|_2^2 = \big((I-\Pi)x\big)^*\mathcal{P}^*\mathcal{P}(I-\Pi)x \quad \begin{cases} \leq \lambda_2\|(I-\Pi)x\|_2^2 \\ \geq \lambda_N\|(I-\Pi)x\|_2^2 \end{cases}$$

as $(I-\Pi)x \perp \mathbf{1}$, where $\mathbf{1}$ is the eigenvector for the largest eigenvalue $\lambda_1 = 1$ of the symmetric matrix $\mathcal{P}^*\mathcal{P}$ whose algebraic and geometric multiplicity is one. □

By Lemma 7 as m becomes large it would be sufficient if we show that the main term of order $1/m$ is nonnegative for the right parameters, i.e., M defined in (3.16) is nonnegative. In the future we plan to derive a lower bound on M. For now we derive a closed form expression for M when $\lambda_2 = 0$. Finally, we will demonstrate that the corresponding parameters regions are nonempty using some sufficiently general classes of distributions (e.g. exchangeable).

Observe that

$$\mathrm{Cov}\left(\mathcal{B}\mu_{\mathsf{x}},\ \Pi X\right) = E\big[\mu_{\mathsf{x}}^*(\mathcal{B}-\Pi)^*\Pi(X-\mu_{\mathsf{x}})\big] = 0 \tag{3.19}$$

as $(\mathcal{B}-\Pi)^*\Pi = 0$.

A closed form expression when $\lambda_2 = 0$. If $\lambda_2 = 0$, then $\mathcal{P} = \Pi$ by Lemma 11,

and

$$\begin{aligned} M &= \mathrm{Var}(X) - \mathrm{Var}(\mathcal{P}X) + \|\mathcal{P}\mu_{\mathrm{x}}\|_2^2 - 2\ \mathrm{Cov}\left(\mathcal{B}\mu_{\mathrm{x}},\ \mathcal{P}X\right) - \mu^*\mu \\ &= \mathrm{Var}(X) - \mathrm{Var}(\Pi X) - \mu^*(I-\Pi)\mu \\ &= E\left[(X-\mu_{\mathrm{x}})^*\big(I-\Pi\big)(X-\mu_{\mathrm{x}})\right] - \delta E\big[Z^*(I-\Pi)Z\big]. \end{aligned} \tag{3.20}$$

Validating. Next, in order to validate the existence of suitable parameters δ, δ'', λ_2, and λ_N for which $M \geq 0$, we consider the following broad classes of distributions.

Case i. Consider a case when

- $\delta = 0 \quad \Leftrightarrow \quad \mu_1 = \mu_2 = \ldots = \mu_N \quad \Leftrightarrow \quad \mu^*(I-\Pi)\mu = 0$;
- $\lambda_2 = 0 \quad \Leftrightarrow \quad \mathcal{P} = \Pi$ (Lemma 11).

This case includes **exchangeable** $Z_1, Z_2, \ldots, Z_N$. Then, substituting $\delta = 0$ into (3.20), we obtain

$$M = E\left[(X-\mu_{\mathrm{x}})^*\big(I-\Pi\big)(X-\mu_{\mathrm{x}})\right] \geq 0$$

and

$$\begin{aligned}\mathcal{E} &= 2\frac{m-1}{m^3}\operatorname{Var}(Z) - \frac{3m-2}{m^3}M - \frac{m-1}{m^3}\mu^*(I-\Pi)\mu \\ &\quad - \frac{m-1}{m^3}\left(\operatorname{Var}(\Pi Z) + \mu_{\mathsf{x}}^*\big(I-\Pi\big)\mu_{\mathsf{x}}\right) \\ &= \frac{m-1}{m^3}\left[\operatorname{Var}(Z) + \operatorname{Var}(Z(I-\Pi)) - \mu_{\mathsf{x}}^*\big(I-\Pi\big)\mu_{\mathsf{x}}\right] - \frac{3m-2}{m^3}M \\ &= \frac{m-1}{m^3}\left[\operatorname{Var}(X) + \operatorname{Var}(Z(I-\Pi)) - \mu^*\big(I-\Pi\big)\mu\right] - \frac{3m-2}{m^3}M \\ &= \frac{m-1}{m^3}\left[\operatorname{Var}(X) + \operatorname{Var}(Z(I-\Pi))\right] - \frac{3m-2}{m^3}E\left[(X-\mu_{\mathsf{x}})^*\big(I-\Pi\big)(X-\mu_{\mathsf{x}})\right].\end{aligned}$$

Then, finally this gives

$$\begin{aligned}\operatorname{Var}(\overline{Z}) - \operatorname{Var}(\overline{Q}) =& \frac{m-1}{m^3}\left[\operatorname{Var}(X) + \operatorname{Var}(Z(I-\Pi))\right] \\ &+ \frac{m^2-3m+2}{m^3}E\left[(X-\mu_{\mathsf{x}})^*\big(I-\Pi\big)(X-\mu_{\mathsf{x}})\right] \geq 0\end{aligned}$$

Notice that for this case Assumption 3 was not used.

Case ii. We consider a case when one ordering of $Z_1, Z_2, \ldots, Z_N$ has probability $\mathbf{p}$, and the other $N! - 1$ orderings all have the same probability smaller than $\mathbf{p}$. Then,

$$\mathcal{P} = \mathbf{a}S + (1-\mathbf{a})\Pi,$$

where S is a permutation matrix corresponding to the likelier ordering, and $\mathbf{a} = \frac{N!\,\mathbf{p}-1}{N!-1}$. In other words,

$$P(\mathcal{B} = S) = \mathbf{p} = \mathbf{a} + \frac{1-\mathbf{a}}{N!},$$

and $N! - 1$ other values of $\mathcal{B}$ each has probability $\frac{1-\mathbf{a}}{N!}$. Then,

$$\mathcal{P}^*\mathcal{P} = \mathbf{a}^2 I + (1 - \mathbf{a}^2)\Pi, \quad \text{and} \quad \lambda_2 = \cdots = \lambda_N = \mathbf{a}^2.$$

Note that since $I - \mathcal{P}^*\mathcal{P} = (1 - \mathbf{a}^2)(I - \Pi)$ then

$$\begin{aligned} \|\mathcal{P}\mu_{\mathsf{x}}\|_2^2 - \mu^*\mu &= \mu_{\mathsf{x}}^* \left(\mathbf{a}^2 I + (1 - \mathbf{a}^2)\Pi\right) \mu_{\mathsf{x}} - \mu^*\mu \\ &= \mathbf{a}^2 \mu_{\mathsf{x}}^* \big(I - \Pi\big)\mu_{\mathsf{x}} - \mu^* \big(I - \Pi\big)\mu, \end{aligned}$$

$$\begin{aligned} \mathrm{Var}(X) - \mathrm{Var}(\mathcal{P}X) &= \mathrm{E}\left[(X - \mu_{\mathsf{x}})^* (I - \mathcal{P}^*\mathcal{P})(X - \mu_{\mathsf{x}})\right] \\ &= (1 - \mathbf{a}^2)\,\mathrm{E}\left[(X - \mu_{\mathsf{x}})^* (I - \Pi)(X - \mu_{\mathsf{x}})\right] \\ &= (1 - \mathbf{a}^2)\left(\mathrm{E}\left[X^* X\right] - \mathrm{E}\left[X^* \Pi X\right] - \mu_{\mathsf{x}}^* \big(I - \Pi\big)\mu_{\mathsf{x}}\right) \\ &= (1 - \mathbf{a}^2)\left(\mathrm{E}\left[Z^*(I - \Pi)Z\right] - \mu_{\mathsf{x}}^* \big(I - \Pi\big)\mu_{\mathsf{x}}\right), \end{aligned}$$

and

$$\begin{aligned} \mathrm{Cov}\left(\mathcal{B}\mu_{\mathsf{x}},\ \mathcal{P}X\right) &= \mathrm{Cov}\left(\mathcal{B}\mu_{\mathsf{x}},\ \ (\mathcal{P} - \Pi)\,X\right) = \mathbf{a}\,\mathrm{Cov}\left(\mathcal{B}\mu_{\mathsf{x}},\ \ (S - \Pi)\,X\right) \\ &\le \mathbf{a}\sqrt{\mu_{\mathsf{x}}^* \big(I - \mathcal{P}^*\mathcal{P}\big)\mu_{\mathsf{x}}\,\mathrm{Var}\left((S - \Pi)X\right)} \\ &= \mathbf{a}\sqrt{(1 - \mathbf{a}^2)\mu_{\mathsf{x}}^* \big(I - \Pi\big)\mu_{\mathsf{x}}\,\mathrm{Var}\left((I - \Pi)X\right)} \\ &= \mathbf{a}\sqrt{(1 - \mathbf{a}^2)\mu_{\mathsf{x}}^* \big(I - \Pi\big)\mu_{\mathsf{x}}\left(\mathrm{E}\left[Z^*(I - \Pi)Z\right] - \mu_{\mathsf{x}}^* \big(I - \Pi\big)\mu_{\mathsf{x}}\right)}. \end{aligned}$$

Then we plug these expressions into our definition of M to find a lower bound.

$$\begin{aligned}
M =& \operatorname{Var}(X) - \operatorname{Var}(\mathcal{P}X) + \|\mathcal{P}\mu_{\mathsf{x}}\|_2^2 - 2\operatorname{Cov}\big(\mathcal{B}\mu_{\mathsf{x}},\ \mathcal{P}X\big) - \mu^*\mu \\
\geq& (1-\mathbf{a}^2)\left(\mathrm{E}\left[Z^*(I-\Pi)Z\right] - \mu_{\mathsf{x}}^*\big(I-\Pi\big)\mu_{\mathsf{x}}\right) + \mathbf{a}^2\mu_{\mathsf{x}}^*\big(I-\Pi\big)\mu_{\mathsf{x}} - \mu^*\big(I-\Pi\big)\mu \\
& - 2\mathbf{a}\sqrt{(1-\mathbf{a}^2)\mu_{\mathsf{x}}^*\big(I-\Pi\big)\mu_{\mathsf{x}}\left(\mathrm{E}\left[Z^*(I-\Pi)Z\right] - \mu_{\mathsf{x}}^*\big(I-\Pi\big)\mu_{\mathsf{x}}\right)} \\
=& \left(\sqrt{(1-\mathbf{a}^2)\left(\mathrm{E}\left[Z^*(I-\Pi)Z\right] - \mu_{\mathsf{x}}^*\big(I-\Pi\big)\mu_{\mathsf{x}}\right)} - \mathbf{a}\sqrt{\mu_{\mathsf{x}}^*\big(I-\Pi\big)\mu_{\mathsf{x}}}\right)^2 \\
& - \delta\,\mathrm{E}\left[Z^*(I-\Pi)Z\right]
\end{aligned}$$

This means M is positive under Assumption 2, and $\operatorname{Var}(\overline{Z}) \geq \operatorname{Var}(\overline{Q})$ for sufficiently large m.

Observe that the two dimensional case $N = 2$ discussed in Section 3.4 would automatically fall into the above class of examples when one ordering of Z_1, Z_2 is likelier than the other.

3.4 Validating assumptions in two-dimensional case

Consider the case when the dimension $N = 2$. Then, equation (3.16) is essential for Theorem 3 (as it is the main term of order $1/m$ in Lemma 7) rewrites as

$$\begin{aligned}
2P(Y>0)P(Y<0)\,\mathrm{E}[Y^2] + 4\Big(P(Y>0) - P(Y<0)\Big)^2\,\mathrm{E}[|Y|]^2 & \\
> \ 5\Big(P(Y>0) - P(Y<0)\Big)\,\mathrm{E}[Y]\,\mathrm{E}[|Y|] + \frac{1}{2}\,\mathrm{E}[Y]^2, &
\end{aligned} \tag{3.21}$$

where $Y = Z_1 - Z_2$.

Next, if we let $Z = \begin{pmatrix} Z_1 \\ Z_2 \end{pmatrix}$ be a Gaussian random vector with mean $\mu = \begin{pmatrix} \mu_1 \\ \mu_2 \end{pmatrix}$ and covariance matrix Σ, then Y is normal with mean $\mu_{\mathsf{y}} = \mu_1 - \mu_2$ and variance

$$\sigma_{\mathsf{y}}^2 = 2 \text{ Var}\big((I - \Pi)Z\big).$$

There, equation (3.21) is equivalent to

$$\begin{aligned} &2\big(1 - \Phi(m_{\mathsf{y}})\big)\Phi(m_{\mathsf{y}})(1 + m_{\mathsf{y}}^2) + 4\Big(2\Phi(m_{\mathsf{y}}) - 1\Big)^2\big(2\Phi'(m_{\mathsf{y}}) + m(2\Phi(m_{\mathsf{y}}) - 1)\big)^2 \\ &> \; 5\Big(2\Phi(m_{\mathsf{y}}) - 1\Big)m_{\mathsf{y}}\big(2\Phi'(m_{\mathsf{y}}) + m(2\Phi(m_{\mathsf{y}}) - 1)\big) + \frac{1}{2}m_{\mathsf{y}}^2, \end{aligned} \tag{3.22}$$

where $m_{\mathsf{y}} = \frac{|\mu_{\mathsf{y}}|}{\sigma_{\mathsf{y}}}$ and $\Phi(x)$ is the standard normal cumulative distribution function. Taking m_{y} to infinity, we observe that the left hand side in (3.22) grows asymptotically as $4\, m_{\mathsf{y}}$, and the right hand side in (3.22) grows asymptotically as $5.5\, m_{\mathsf{y}}$. Thus, (3.22) is not satisfied for large magnitudes of $m_{\mathsf{y}} = \frac{|\mu_{\mathsf{y}}|}{\sigma_{\mathsf{y}}}$. At the same time, plugging in $m_{\mathsf{y}} = 0$, we obtain that the equation (3.22) is valid in a neighborhood of zero. So, we conclude that Theorem 3 is valid if and only if

$$m_{\mathsf{y}} = \frac{|\mu_{\mathsf{y}}|}{\sigma_{\mathsf{y}}} = \left\| \frac{E\big[(I - \Pi)Z\big]}{\sqrt{\text{Var}\big((I - \Pi)Z\big)}} \right\|_2$$

is sufficiently small, confirming the necessity of the Assumption 2 for Theorem 3.

4 Assessing monotonicity in biological networks

4.1 Background

Following [13, 14], covariance graphs with edges in the form of dashed or discontinuous lines are typically used to describe the marginal independence structure among a set of Gaussian random variables. They are distinct from the concentration graphs (or inverse covariance graphs) that are traditionally understood in terms of the Markov property. Covariance graphs have received a fair amount of attention in works by [8], [17], [29], [9], [18], [4], [38], [20], and many others. Specifically, [20] provides a dual likelihood method and MIM algorithm for estimation. A practical multiple testing-based approach to model selection is discussed by [17]. Another development was the [18] derivation of an iterative algorithm for maximum likelihood estimation. [8] and [29] advanced applications in biological sciences.

We are particularly interested in changes (including phase transitions) in a biological network that happen during a normal cell differentiation process as well as in the development of a disease (e.g., cancer) or infection. When a biological system transits from one state to another, changes occur in the amounts of messenger RNAs, proteins, metabolites, and other biological units. These changes represent a cascade of interactions controlling different biological pathways, providing infor-

mation about the underlying structure of regulatory relations between biological units. The idea is that if we observe different levels of a given molecule (e.g. gene expression) in different states we may be able to ignore the feedback regulatory mechanisms as they were not sufficient to control the molecule, and, in such instances, much of the network can become interpretable in terms of causal relations. In other words, it is thought that changes in amounts of different molecules during biological transitions would be a much more common event than alterations in biochemical/physical interactions between molecules. For further references on biological networks, see e.g. [64, 33]. It has been found that many biological networks should largely adhere to the following inequalities,

$$(\mu_{0,v} - \mu_{1,v})(\mu_{0,v'} - \mu_{1,v'})\rho_{0,v,v'} > 0, \quad (\mu_{0,v} - \mu_{1,v})(\mu_{0,v'} - \mu_{1,v'})\rho_{1,v,v'} > 0, \quad (4.1)$$

that are linked with these causal relations.[67] The objective here is to utilize statistical tests to build covariance graphs and assess adherence to these inequalities. The details of these tests and their multiplicity corrections are discussed in the chapter. The procedure also allows us to control family-wise error rate or false discovery rate and to select covariance graphs. We also report analysis of two studies that compare gene expressions between healthy (no cancer) and cancer tissues. The analysis suggests that for both studies, underlying biological networks largely follow the inequalities in (4.1).

The causal relationships are due to a probabilistic monotonicity property of certain covariance graphical models. Several notions of monotonicity have been pos-

tulated in the works of [32], [66], [19], [6], [46], [62] and more recently in [63], [15], [40] and [67]. In probability theory and statistical mechanics, monotonicity, however, corresponds to the notion of increasing and decreasing random variables and related correlation inequalities that emerged in the study of Ising, Potts, and percolation models and other statistical mechanical systems. The Fortuin-Kasteleyn-Ginibre (FKG) inequality [25] and the closely related concept of multivariate total positivity of order 2 [36] explain most of the results involving monotone random variables and monotone (increasing or decreasing) events.

Figure 4.1 plots examples of covariance graphs with 6 nodes where the networks on the left possess this monotonicity property defined by the FKG inequalities in (4.1). Here the top graph (A) is from state 1 (e.g. healthy patients) and the bottom graph (C) is from state 0 (e.g. sick patients). However, the monotonicity property is violated in Figure 4.1 by covariance graphs plotted on the right. Specifically, for graphs on the right, the covariance between variables at node 1 and 2 are negative and thus defies (4.1). Furthermore, the edge between nodes 3 and 4 in graph (B) also violates (4.1).

The biological interpretation of the inequalities in (4.1) can be given via the common cause principle which states that, in the absence of a feedback loop, if X_v and $X_{v'}$ are to be correlated we must either have that (1) X_v regulates $X_{v'}$, (2) $X_{v'}$ regulates X_v, (3) there is a common cause that regulates both X_v and $X_{v'}$ or (4) the correlation is attributed to noise in the network [45, 54]. Thus, within one biological state, positive correlations are to be found between the pairs of up/up-regulated genes and the pair of down/down-regulated genes. Similarly,

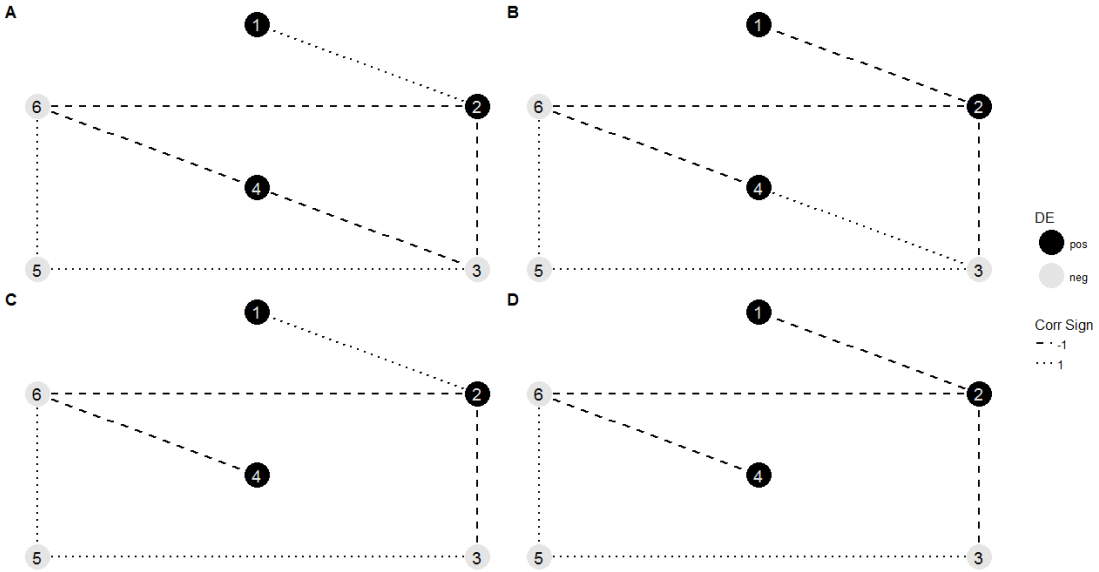

Figure 4.1: Examples of networks where the networks on the left (right) possess (lack) the monotonicity property defined by the FKG inequalities in (4.1). The top graphs are from state 1 (e.g. healthy patients), and the bottom graphs are from state 0 (e.g. sick patients). Dark (light) nodes represent genes who are positively (negatively) differentially expressed. Dashed (dotted) lines represent negative (positive) correlation between the connected genes.

negative correlations are to be found between pairs of up/down-regulated genes. Correlations that do not follow the above rule are the unexpected correlations we can attribute to the noise in the system or to the presence of a feedback loop.

In practice, however, we observe two (normalized) random samples of (noisy) log-gene expressions, namely, $y_{0,v,i}$, $v \in \mathcal{V}$, $i = 1, 2, \ldots, n_0$ and $y_{1,v,i'}$, $v \in \mathcal{V}$, $i' = 1, 2, \ldots, n_1$, where $\mathcal{V} = \{1, 2, \ldots, m\}$ and m is the total number of genes. Here the first sample is collected from n_0 individuals at state 0 and the second sample is taken from n_1 individuals at state 1. Let $Y_{0,v,i}$ and $Y_{1,v,i'}$ denote the random

variables whose realizations are $y_{0,v,i}$ and $y_{1,v,i'}$. Necessarily, we set

$$\mathrm{E}[Y_{0,v,i}] = \mu_{0,v}, \quad \mathrm{E}[Y_{1,v,i'}] = \mu_{1,v},$$

and

$$corr(Y_{0,v,i}, Y_{0,v',i}) = \rho_{0,v,v'}, \quad corr(Y_{1,v,i'}, Y_{1,v',i'}) = \rho_{1,v,v'}.$$

If the noise level is small or negligible, the monotonicity property of X_v, $v \in \mathcal{V}$ will be preserved in $Y_{0,v,i}$ and $Y_{1,v,i'}$, $v \in \mathcal{V}$, $i = 1, 2, \ldots, n_0$, $i' = 1, 2, \ldots, n_1$ and we shall still have (4.1). On the other hand, when the noise is substantial in the observed log-gene expression or when there is a presence of a feedback loop, the above expected correlation inequalities can be violated. The question then becomes how we can statistically assess to the extent to which there is empirical evidence of the monotonicity property (4.1) in the observed gene-expression or other observed biological networks. Furthermore, if the monotonicity assumption is reasonable, another important problem is to select covariance graphs under 4.1. To this end, we consider (4.1) and a sequence of tests on means $\mu_{0,v}, \mu_{1,v}$ and correlations $\rho_{0,v,v'}, \rho_{1,v,v'}$ with multiplicity corrections. In the next section, we provide details of these tests along with normalization that reduces unwanted variations to some extent.

4.2 Statistical Methods

4.2.1 Normalization

Gene expression data are generally normalized to reduce unintended but systematic variations of non-biological origins and to improve comparability. Typically observed gene expressions include not just biological information such as mean differences in the expression of particular genes between an unhealthy (or sick) tissue and a healthy (or normal) tissue or information on dependence structures among genes, but also non-biological variations that are introduced while collecting and processing the samples. Sources of these variations are many including changes in substrate surface characteristics, cross-linking effects, cDNA library selection and amplification, hybridization kinetics and thermodynamics, and probe deposition technology. The works of [30], [1], [49], [7], [55], [61], [24], [34], and many subsequent articles provide a significant discussion on this topic and present numerous statistical methods of performing the normalization.

In the simplest case, normalization is done via suitable scaling of the intensities so that each array has the same average value or by transforming the data so that the distribution of intensities is the same across a set of arrays. In complex cases, normalization requires sophisticated adjustments and combining information from all gene expression arrays where the intention is to bring the entire set of probability distributions of adjusted values into alignment. For example, the median normalization divides all gene observations for a subject by the value of the median observation for that subject. It does not account for location effects,

including groups of genes with common measurement error issues. Similarly, quantile normalization begins by determining ranks of gene expression measurements for each subject. Then ordering observations by rank for each subject and finding the average value for each order statistic. For example, let $\ell_{0,i}(v)$ be the rank of $f_{0,v,i}$ and $\ell_{1,i}(v)$ the rank of $f_{1,v,i}$, where $f_{0,v,i}$ and $f_{1,v,i}$ are the raw gene expression levels of the vth gene for the ith subject within states 0 and 1, respectively. Then,

$$y_{0,v,i} = \log_2 \left[\frac{\sum_{i'=1}^{n_0} f_{0,\left(\ell_{0,i}(v)\right),i'}}{n_0} \right], \quad y_{1,v,i} = \log_2 \left[\frac{\sum_{i'=1}^{n_1} f_{1,\left(\ell_{1,i}(v)\right),i'}}{n_1} \right],$$

where $v = 1, \ldots, m$ and $f_{0,(1),i'} \leq f_{0,(2),i'} \leq \ldots \leq f_{0,(m),i'}$. As an example, $y_{0,3,2}$ is the logged gene expression of the 3rd gene for the 2nd individual in state 0, and $\ell_{0,2}(3)$ is the rank of $f_{0,3,2}$ among all $f_{0,v,2}$'s. However, quantile normalization is not as robust to outliers and errors in the data as rank normalization. Rank normalization also begins by determining ranks of gene expression measurements for each subject. Then those ranks are divided by the total number of genes per subject, $y_{0,v,i} = \ell_{0,i}(v)/m$ and $y_{1,v,i} = \ell_{1,i}(v)/m$. This method loses some parametric information that quantile normalization does not. LOWESS normalization uses a reference array, $z_v, v \in \mathcal{V}$, to find the ratio and product for each subject. Then create a scatter plot of $\log_2(f_{0,v,i}/z_v)$ values versus the $\log_2(f_{0,v,i}\, z_v)/2$ values for $v = 1, ..., m$. Then subtract a lowess fitted function of this data from $\log_2(f_{0,v,i})$.

We will use quantile normalization in Section 3.2, and rank normalization in Section 3.3. Unlike [17], which focused on Šidák inequalities to control the family-wise error rate, we apply multiplicity corrections to control false discovery rates

and select covariance graphs.

4.2.2 Two stage t-test procedure

In this subsection, we assume that normalized log gene expressions $y_{0,v,i}$, $v \in \mathcal{V}$, $i = 1, 2, \ldots, n_0$ and $y_{1,v,i'}$, $v \in \mathcal{V}$, $i' = 1, 2, \ldots, n_1$ are realizations of Gaussian random variables and focus on assessing the monotonicity property described in equations (4.1). It is desirable to ensure that differences in the average gene expressions are due to the change of biological state being studied. Furthermore, equations (4.1) suggest that finding the most statistically significant differences in the average gene expressions should be the first step. With this in mind, we can state null and alternative hypotheses of the form

$$H_v : \ \mu_{0,v} - \mu_{1,v} = 0 \ , \quad \text{and} \quad K_v : \ \mu_{0,i} - \mu_{1,i} \neq 0, \quad v \in \mathcal{V}. \tag{4.2}$$

Since the number of subjects in each state (e.g. normal, diseased) are not necessarily balanced and we make no assumptions on the variability of the log gene expressions, we can use a Welch's t-test [65] to find the significance level of each mean gene expression difference. A 2-sided p-value, $p_v^{(1)}$, is found for each gene v using the following equations

$$t_v^{(1)} = \frac{\bar{y}_{0,v} - \bar{y}_{1,v}}{\sqrt{\frac{s_{0,v}^2}{n_0} + \frac{s_{1,v}^2}{n_1}}} \ , \qquad d_v = \frac{\left(\frac{s_{0,v}^2}{n_0} + \frac{s_{1,v}^2}{n_1}\right)^2}{\frac{(s_{0,v}^2/n_0)^2}{n_0 - 1} + \frac{(s_{1,v}^2/n_1)^2}{n_1 - 1}} \ ,$$

and

$$p_v^{(1)} = 2\,P(T_{d_v} \geq |t_v^{(1)}|)\ , \tag{4.3}$$

where $\bar{y}_{0,v}$, $s_{0,v}$, $\bar{y}_{1,v}$ and $v_{0,v}$ are respectively the sample means and the sample standard deviations of $y_{0,v,i}$, $i = 1, 2, \ldots, n_0$ and $y_{1,v,i'}$, $i' = 1, 2, \ldots, n_1$ for gene v, and T_{d_v} is a t random variable with d_v degrees of freedom.

Since we are effectively doing a multiple comparison across thousands or tens of thousands of genes, we consider two methods to control the false discovery rate (FDR): the Benjamini-Hochberg-Yekutieli (BHY) procedure [3] and empirical null modelling [21]. The first method requires positive regression dependence, which is achieved when the inequalities in (4.1) hold. The second method does not require any form of dependence or independence and is less conservative.

To use the BHY procedure, first let $\ell(v)$ be the rank of $p_v^{(1)}$. Then the procedure has us find the largest $\ell(v)$ such that

$$p_v^{(1)} \leq \frac{\ell(v)}{m\,c(m)}\alpha, \quad c(j) = \sum_{v=1}^{j} v^{-1} \approx \log(j) + \gamma + \frac{1}{2j}, \quad j \geq 1, \tag{4.4}$$

where γ is the Euler-Mascheroni constant. We can rearrange this formula to get $m\,c(m)p_v^{(1)}/\ell(v) \leq \alpha$. The quantity on the left can be calculated for each gene and compared to a given value of α. Let k be the largest value of $\ell(v)$ that fulfills the inequality and thus the number of genes that will be considered going forward. Then we can define the set

$$\mathcal{V}_1 = \{v\ :\ 1 \leq \ell(v) \leq k\}.$$

Alternatively, empirical null modelling[22] will be used to calculate an adjusted p-value which can be compared directly to the desired α level. The method is inspired by use of an Empirical Bayes framework. The method is described and the resulting formula for the adjusted p-values is derived in Appendix A. The formula for the adjusted p-value that is found is

$$p_{v,E}^{(1)} = FDR_0(z_v)\left[1 + \hat{A}\frac{z_v\phi(z_v)}{\sqrt{2}(1-\Phi(z_v))}\right],$$

where $FDR_0(z_i) = N(1-\Phi(z_i))/\left(\sum_j z_j \geq z_i\right)$ would be the unconditioned (ie, assuming independence) estimate of the FDR under the null hypothesis. Thus, an alternative definition of $\mathcal{V}_1$ would be

$$\mathcal{V}_1 = \{v \ : \ p_{v,E}^{(1)} \ \leq \ \alpha\}.$$

For a given choice of a large-scale significance testing method, all genes $v \in \mathcal{V}_1$ will be considered to be expressed significantly different enough in the two states to include in the network. This is equivalent to rejecting the null hypothesis that these genes do not express differently in the two different states.

At this point, we have the k_1 most probable candidates for a network of genes that should be somehow involved in the mechanism of changing from one state to another. Now we identify our null and alternative hypotheses on correlations for state 0 as follows

$$H_{0,v,v'} : \ \rho_{0,v,v'} = 0 \ , \quad \text{and} \quad K_{0,v,v'} : \ \rho_{0,v,v'} \neq 0, \quad v, v' \in \mathcal{V}_1. \tag{4.5}$$

Similarly, we define $H_{1,v,v'}$ and $K_{1,v,v'}$, for $v, v' \in \mathcal{V}_1$ that cover the correlation inequalities at state 1.

To test these hypotheses, we first calculate the sample correlations between $y_{0,v,i}$ and $y_{0,v',i}$ for $i = 1, 2, \ldots, n_0$ and between $y_{1,v',i'}$, and $y_{1,v',i'}$ for $i' = 1, 2, \ldots, n_1$ for every possible pair of genes $v, v' \in \mathcal{V}_1$, i.e.,

$$r_{0,v,v'} = \hat{cor}(Y_{0,v}, Y_{1,v'}) \ , \quad \text{and} \quad r_{1,v,v'} = \hat{cor}(Y_{1,v}, Y_{1,v'}).$$

Next, we calculate the t-statistic [52] for significance of a correlation coefficient and the corresponding two-sided p-value. For state 0:

$$t^{(1)}_{0,v,v'} = r_{0,v,v'} \sqrt{\frac{n_0 - 2}{1 - r^2_{0,v,v'}}} \ , \quad \text{and} \quad p^{(1)}_{0,v,v'} = 2\, P(T_{n_0-2} \geq t^{(1)}_{0,v,v'}). \tag{4.6}$$

For state 1:

$$t^{(1)}_{1,v,v'} = r_{1,v,v'} \sqrt{\frac{n_1 - 2}{1 - r^2_{1,v,v'}}} \ , \quad \text{and} \quad p^{(1)}_{1,v,v'} = 2\, P(T_{n_1-2} \geq t^{(1)}_{1,v,v'}). \tag{4.7}$$

Once again, we are faced with a large scale multiple comparison. If we choose to control the false discovery rate through use of the Benjamini-Hochberg-Yekutieli procedure for the same reasons, then the full list of all possible pairs of genes is then sorted by the calculated p-value (smallest to largest). As before, we look for the largest $\ell(v, v')$ such that

$$p^{(1)}_{0,v,v'} \frac{m^*}{\ell(v, v')} \leq \alpha, \quad m^* = \{k(k-1)/2\}\, c\Big(k(k-1)/2\Big), \tag{4.8}$$

where $\ell(v, v')$ is the rank of the p-value, $p^{(1)}_{0,v,v'}$, in the list, and m^* depends only on the total number of possible pairs. If instead we control the false discovery rate by utilizing Efron's method, then the only change will be that $z_v = \Phi^{-1}\left(1 - p^{(1)}_{0,v,v'}\right)$ and the procedure will follow as before. Either method will produce a set of gene pairs that will be considered to be significantly correlated enough for the corresponding edge to remain in the network. This is equivalent to rejecting the null hypothesis that these genes are uncorrelated. Significant p-values allow us to select covariance graphs in similar ways as [17].

4.2.3 Two stage rank test procedure

The t-tests used in the previous subsection assume that the data is normally distributed. An argument could be made that this is not strictly true. Combined with small sample sizes, which are not uncommon with gene expression data, this could call into question the use of t-distribution based methods. To address this contingency, non-parametric rank based tests are considered. A thorough overview of rank based procedures can be found in [59].

The data first undergoes a rank normalization. This means that observations for each subject are separately ranked and those ranks are then divided by the total number of genes per subject. Then, to find the differentially expressed genes, the Wilcoxon Mann-Whitney rank-sum test [41] is performed, and a p-value obtained, on the data for each gene. The alternative hypothesis being tested is that the distribution of one sample stochastically dominates the other. The first step in the

test is for all observations, $y_{0,v,i}$ for $i = 1, 2, \ldots, n_0$ and $y_{1,v,i'}$ for $i' = 1, 2, \ldots, n_1$, from a particular gene to be ranked based on their value regardless of which state it comes from. Then the ranks for each sample (state) are added up. Let these rank sums be $g_{0,v}$ and $g_{1,v}$. Then our test statistics are

$$u_{0,v} = g_{0,v} - \frac{1}{2}n_0(n_0 + 1) \quad \text{and} \quad u_{1,v} = g_{1,v} - \frac{1}{2}n_1(n_1 + 1).$$

However, $u_{0,v} + u_{1,v} = n_0 n_1$, therefore, we only need either $u_{0,v}$ or $u_{1,v}$. A p-value can be calculated exactly by randomization test (for sufficiently small sample sizes), by normal approximation, or by use of a simulated null distribution. An approximation by way of t-distribution [11] is also possible but not explored here.

For our data, and most realistic data, sample sizes will often be large enough to make an exact calculation impractical. Let $\nu = \frac{1}{2}n_0 n_1$ and $\sigma^2 = \{n_0 n_1(n_0 + n_1 + 1)\}/12$. If a normal approximation is to be used, then the p-value is

$$p_v^{(2)} = 2\left(1 - \Phi\left(\left|\frac{u_{0,v} - \nu}{\sigma}\right|\right)\right). \tag{4.9}$$

If instead, a simulated null distribution is used, then a randomized p-value [12] can be found by randomly selecting a p-value from a uniform distribution from $q_{v,-}^{(1)}$ to $q_v^{(1)}$ where

$$q_{v,-}^{(1)} = \frac{1}{B}\sum_{b=1}^{B} I\left(\left|U^{(b)} - \nu\right| > |u_{0,v} - \nu|\right), \tag{4.10}$$

where $U^{(b)}$, $b = 1, 2, \ldots, B$ are the B simulated rank-sum statistics from the null

distribution and

$$q_v^{(1)} = \frac{1}{B}\sum_{b=1}^{B} I\left(\left|U^{(b)} - \nu\right| \geq |u_{0,v} - \nu|\right).$$

In the vast majority of cases when the number of genes is fairly large, the difference between $q_v^{(1)}$ and $q_{v,-}^{(1)}$ is so small that simply using $q_v^{(1)}$ will effectively give the same result as a randomized p-value.

The Benjamini-Hochberg-Yekutieli procedure or Efron's method is then performed using each set of these p-values in the exact same way as the t-based procedure. The randomized p-values are selected many times and a suitable cutoff is used for rejection probabilities from these selections. This will result in two sets ($\mathcal{V}_2$ for the normal approximation, $\mathcal{V}_3$ for a simulated null distribution) of network candidate genes. The next step is to find significant gene-gene correlations.

Let $\mathcal{V}_2$ be the set of genes (consisting of k_2 candidates) that are selected via the Benjamini-Hochberg-Yekutieli procedure with rank-sum tests using a normal approximation. Similar hypotheses related to significant correlations, (4.5), will be tested now. To be precise, we shall test the hypotheses

$$H_{0,v,v'}: \ \varrho_{0,v,v'} = 0\ , \quad \text{and} \quad K_{0,v,v'}: \ \varrho_{0,v,v'} \neq 0, \quad v, v' \in \mathcal{V}_2,$$

and

$$H_{1,v,v'}: \ \varrho_{1,v,v'} = 0\ , \quad \text{and} \quad K_{1,v,v'}: \ \varrho_{1,v,v'} \neq 0, \quad v, v' \in \mathcal{V}_2,$$

where $\varrho_{0,v,v'}$ and $\varrho_{1,v,v'}$ denote the Spearman rank correlations between $Y_{0,v,i}$ and $Y_{0,v',i}$ and between $Y_{1,v,i}$ and $Y_{1,v',i}$, respectively. We will first calculate the sample

Spearman rank correlation which is same as the sample Pearson correlation of the ranks [43]. This means that once we have p-values, the same multiple testing procedure for correlations from the t-based method can be used [37], though it will be an approximation and not an exact p-value. For the t approximation, we can specifically use:

$$t^{(2)}_{0,v,v'} = u_{0,v,v'}\sqrt{\frac{n_0-2}{1-u^2_{0,i,i'}}}\ , \quad \text{and} \quad p^{(2)}_{0,v,v'} = P(T_{n_0-2} \geq t^{(2)}_{0,v,v'}) \tag{4.11}$$

and

$$t^{(2)}_{1,v,v'} = u_{1,v,v'}\sqrt{\frac{n_1-2}{1-u^2_{1,v,v'}}}\ , \quad \text{and} \quad p^{(2)}_{1,v,v'} = P(T_{n_1-2} \geq t^{(2)}_{1,v,v'}). \tag{4.12}$$

where $u_{0,v,v'}$ and $u_{1,v,v'}$ are now the sample Spearman correlations between $y_{0,v,i}$ and $y_{0,v',i}$ for $i = 1, 2, \ldots, n_0$ and between $y_{1,v',i'}$, and $y_{1,v',i'}$ for $i' = 1, 2, \ldots, n_1$ for every possible pair of genes $v, v' \in \mathcal{V}_2$. For the use of a randomized p-value from a simulated distribution, we can use

$$q^{(2)}_{0,v,v',-} = \frac{1}{B}\sum_{b=1}^{B} I\left(U_0^{(b)} < u_{0,v,v'}\right)$$

and

$$q^{(2)}_{0,v,v'} = \frac{1}{B}\sum_{b=1}^{B} I\left(U_0^{(b)} \leq u_{0,v,v'}\right)$$

in the same way as with the differentially expressed genes, where $U_0^{(b)}$, $b = 1, 2, \ldots B$ are the simulated rank correlations under the independence assumption. Once

again the same Benjamini-Hochberg-Yekutieli procedure or Efron's method is used for each set (for each method: normal approximation, simulated null distribution) of gene pairs. As with the tests for differential expression, if $q^{(2)}_{0,v,v',-}$ and $q^{(2)}_{0,v,v'}$ have values very close to each other, we can simply use $q^{(2)}_{0,v,v'}$, which will effectively give the same result as the randomized p-values.

4.3 Analysis

4.3.1 Analysis of data from [42]

[42] analyzed a gene expression dataset consisting of expression measurements from 1,844 probes measured on 54 subjects. Each probe corresponds to a gene and there are a handful of genes that are mapped to by 2 probes. The study actually comprises a total of 14,784 probes, but only 1844 probes have measurements for all subjects. The majority of the discarded probes have very few observations in at least one state. Clearly we will not be able to draw any conclusions about the part of the network containing the genes (nodes) with missing observations that we exclude from our analysis. However, since (4.1) is based only on the observations at the node and pairwise computations for two nodes v and v', then we can analyze the region of the network containing the genes with no missing observations. This data comes from a meta-analysis of gene expression and chromosomal aberration studies containing 20 healthy patients and 34 patients with cervical cancer.

We perform Welch's t-test on each probe and control for the FDR by using

the Benjamini-Hochberg-Yekutieli procedure as described in Section 4.2.2. At an $\alpha = 0.05$ level, 201 genes are found to be differentially expressed. However, in each case α will be chosen so that a similar number of genes are found to be differentially expressed. Interestingly, none of the genes that are mapped to 2 probes are found to be differentially expressed.

From k_1 genes selected as differentially expressed, we next calculate all pairwise correlations, $r_{0,v,v'}$ and $r_{1,v,v'}$, with $v, v' \in \mathcal{V}_1$. Therefore, each state will have $k_1(k_1 - 1)/2$ unique calculated values representing pairwise correlations for each state. For the $k_1 = 134$ ($\alpha = 0.0032$) differentially expressed genes (all remaining probes mapped to unique genes) that are detected, we then have $8,911$ pairs of correlations that we test according to inequalities (4.1) in Section 4.1. Pairs of correlations involving at least one gene that was not found to be differentially expressed are not considered, since we would not know if the measured differences are truly positive or negative.

As described in Section 4.2.2, we performed t-tests on a certain function, (4.6) and (4.7), of the Pearson's correlation coefficient, and the FDR is once again controlled through use of the Benjamini-Hochberg-Yekutieli procedure. In Figure 4.2A we have a covariance graph built from the most significantly differentially expressed genes ($\alpha = 0.0032, 134$ genes) of the 1,844 complete genes of the data from [42]. Dark nodes are genes displaying positive differential expression (higher mean expression in sick group) and the light nodes are genes displaying negative differential expression. Edges exist for significant correlations within the healthy subjects data. The sign of the correlation (along with the direction of the dif-

ferential expressions) determines whether an edge is expected according to the FKG inequalities in (4.1). In this network all 55 existing edges are expected (0.0% unexpected). There are a few small sub-networks (2-3 genes) and two larger sub-networks that are mostly segregated by the direction of differential expression. A large proportion of these edges (90.9%) correspond to a positive correlation, since the sub-networks present mostly contain genes with the same sign of differential expression.

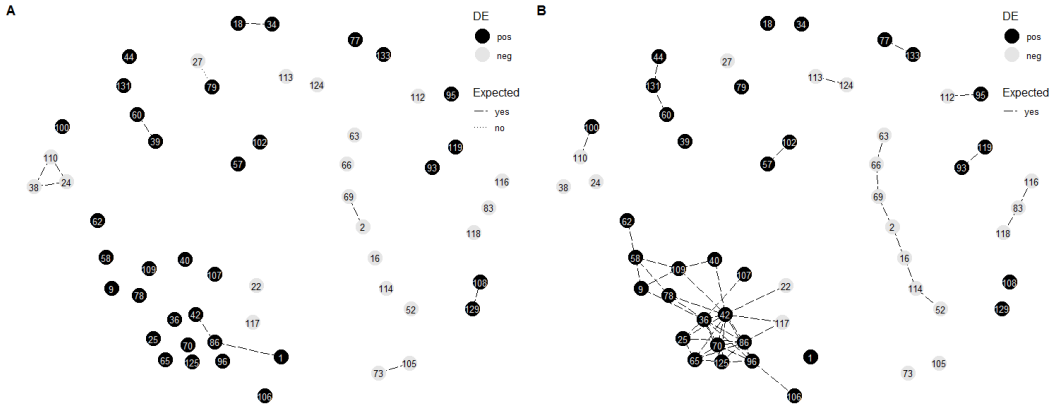

Figure 4.2: Covariance graphs built using t-test based methods for A)healthy patients and B)cancer patients from [42]. Dark (light) nodes represent genes who are positively (negatively) differentially expressed. Dashed (dotted) lines represent expected (unexpected) correlation between the connected genes. The labels on the nodes denote the rank of the p-value of the t-test of differential expression. Nodes with no significant edges are excluded for ease of viewing. $\alpha = 0.0032, \alpha' = 0.05$

Figure 4.2B shows a covariance graph built in the same way from the same data, but using the sick patients. In this network 10 of the 11 existing edges are expected. The only unexpected edge corresponds to a pair of genes with opposite signs of differential expression that are positively correlated. Otherwise all of the

other very small (2-3 genes) sub-networks contain genes with the same sign of differential expression. This means all edges correspond to negatively correlated genes.

Biologists generally believe that the unexpected edges are the result of either noise in the system or the presence of a feedback mechanism. In either case, the edge is not considered to be related to the difference in state, and thus if one desires to create a gene regulatory network that describes the state change, these edges would not be included in the network.

The very low proportion of significant negative correlations seen in these two covariance graphs could be a result of normalization issues. This can cause some bias toward positive correlations, which is explained further in the Appendix.

When using the rank based procedure with a normal approximation on the data from [42], we come up with $k_2 = 137$ ($\alpha = 0.02$) differentially expressed genes (all remaining probes again mapped to unique genes). The α here is chosen higher (rank test has less power than the t-test) to give a similar number of genes as yielded in the graphs built by using t-tests. This is done with Mann-Whitney U tests on each gene and by controlling the FDR by once again using the Benjamini-Hochberg-Yekutieli procedure as described in Section 4.2.2. Once again, the rank tests didn't detect any differentially expressed genes that are mapped to 2 probes. This results in $9,316$ pairs of correlations. Figure 4.3A shows a covariance graph built using the rank based procedure with data from [42] and using the healthy patients. In this network, all of the 25 edges are expected (0.0% unexpected). Again, a large majority (88.0%) of edges represent positively correlated gene pairs.

Many of the edges present are also present in figure 4.2A. However, due to the higher power of the correlation t-test, there are numerous edges in figure 4.2A that are not present in figure 4.3A.

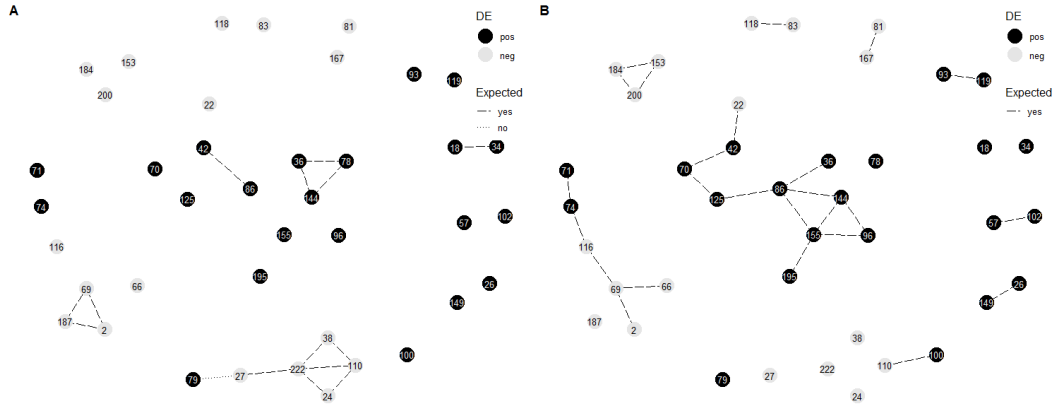

Figure 4.3: Covariance graphs built using rank test based methods for A)healthy patients and B)cancer patients from [42]. Dark (light) nodes represent genes who are positively (negatively) differentially expressed. Dashed (dotted) lines represent expected (unexpected) correlation between the connected genes. The labels on the nodes denote the rank of the p-value of the t-test of differential expression. Nodes with no significant edges are excluded for ease of viewing. $\alpha = 0.02, \alpha' = 0.05$

Figure 4.3 also shows a covariance graph built with data from [42] but using the sick patients. In this network, all but one of the 15 edges are expected. All sub-networks have like signs of differential expression except for one node connected by the unexpected edge. This means all 15 edges correspond to positively correlated gene pairs. Again, many of the edges present are also present in figure 4.2B, and there are numerous edges in figure 4.2B that are not present in figure 4.3B.

Table 4.1: Number of genes found to be differentially expressed using four different methods.

Data	α	BHY	Efron	locfdr	fdrtool
[42]	0.003152	134	189	303	136
[42]	0.05	340	531	748	311
[58]	10^{-8}	134	130	226	275

Table 4.2: The α levels used for each set of tests and the resulting number of genes found to be differentially expressed.

Data	Method	BHY α	Efron α	# DE
[42]	t	0.003152	0.000156	134
[42]	rank	0.02008	0.001036	137
[58]	t	$9.8032 * 10^{-9}$	$3.7489 * 10^{-10}$	134
[58]	rank	$8.0977 * 10^{-6}$	$7.2621 * 10^{-9}$	134

Table 4.3: The number of genes found to be differentially expressed when $\alpha = 0.01$ when using empirical null modelling.

Data	Method	# DE
[42]	t	534
[42]	rank	400
[58]	t	6379
[58]	rank	6043

4.3.2 Analysis of data from [58]

A second dataset from [58], consisting of 22,278 probes measured on 57 subjects was also analyzed. Each probe corresponds to a gene and there are $4,353$ genes that are mapped to more than one probe. The study comprised of $22,283$ total probes but only 22,278 probes have measurements for all subjects. With only five probes with missing observations, we remove them from the analysis as done in Section 4.3.1. This data comes from a study that explored the role of genes on chromosome arm 20q in the progression of cervical cancer. The exact number of differentially expressed probes using the t-based method is $k_1 = 134$; we then have $8,911$ pairs of correlations that we wish to test according to the inequalities in (4.1) in Section 4.1.

Figure 4.4A shows a covariance graph built in the same way as with Figure 4.2 but with data from [58] and using the healthy patients. In this network 315 of the 339 existing edges are expected (7.1% unexpected). There are a few small sub-networks (2-4 genes) and one large sub-network that is mostly segregated by the direction of differential expression. In fact, there are only a handful of expected edges connecting the groups within the sub-network. This means that the large majority (81.4%) of edges represent positively correlated pairs of genes. For the same reasons argued in Section 4.3.1, we can consider ignoring the unexpected edges. This reinforces the segregation of the genes with positive and negative differential expression.

Figure 4.4B also shows a covariance graph built with data from [58] but using

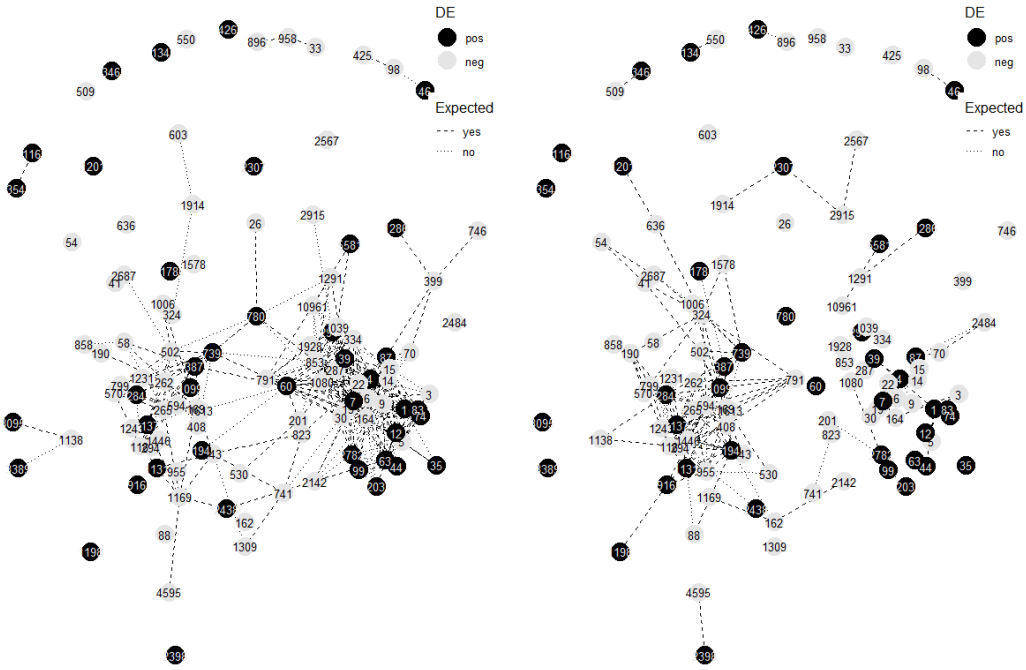

Figure 4.4: Covariance graphs built using t-test based methods for A)healthy patients and B)cancer patients from [58]. Dark (light) nodes represent genes who are positively (negatively) differentially expressed. Dashed (dotted) lines represent expected (unexpected) correlation between the connected genes. The labels on the nodes denote the rank of the p-value of the t-test of differential expression. $\alpha = 10^{-8}, \alpha' = 0.05$

the sick patients. In this network all 154 existing edges are expected (0.0% unexpected). All sub-networks, with the exception of one with 3 genes, have like signs of differential expression. This means all but two of the 154 edges correspond to positively correlated gene pairs.

When using the rank based procedure with normal approximations on the data from [58], we come up with $k_2 = 134$ differentially expressed genes. This results in $8,911$ pairs of correlations. Figure 4.5 shows a covariance graph built using the

rank based procedure with data from [58] and using the healthy patients. In this network, all but one of the 252 edges are expected (0.4% unexpected). Again, a large majority (83.7%) of edges represent positively correlated gene pairs.

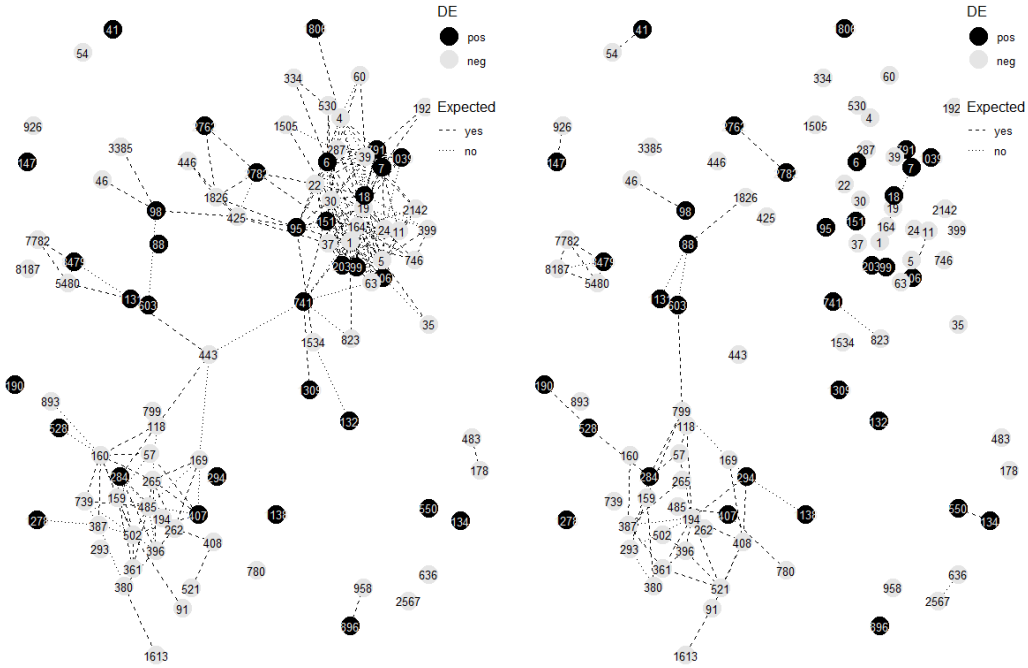

Figure 4.5: Covariance graphs built using rank test based methods for A)healthy patients and B)cancer patients from [58]. Dark (light) nodes represent genes who are positively (negatively) differentially expressed. Dashed (dotted) lines represent expected (unexpected) correlation between the connected genes. The labels on the nodes denote the rank of the p-value of the t-test of differential expression. Nodes with no significant edges are excluded for ease of viewing. $\alpha = 8 \times 10^{-6}, \alpha' = 0.05$

Figure 4.5B also shows a covariance graph built with data from [58] but using the sick patients. In this network all 57 existing edges are expected (0.0% unexpected). All sub-networks have like signs of differential expression. This means all 57 edges correspond to positively correlated gene pairs.

It should be noted that in either test only 24 of the probes that map to non-unique genes are found to be differentially expressed. Although figure 4.4 is drawn using some of these probes, typically biologists follow certain predefined procedures for choosing which probe to represent a specific gene.

4.4 Discussion

In this chapter, we have discussed a probabilistic monotonicity property as biological networks transit from one state to another. The notion of monotonicity allows for causal interpretation of biological networks. It is believed that networks are interpretable in terms of causal relations under the assumptions that 1) gene-gene interaction can be either a stimulation or an inhibition, 2) the regulatory relations hold across different states of a biological system, and 3) if we observe different levels of gene expression in different states we can ignore the feedback regulatory mechanisms as they were not sufficient to control the molecule. While these assumptions cannot hold across all possible biological processes, they seem to represent common features of various biological systems, particularly those for which the sample space can be represented by a distributive lattice with a partial order.

Though limited in sample size, individual statistical tests on means and correlations with multiplicity corrections seem to be one useful concept by which we can assess the monotonicity property. The unexpected correlations, following our data examples, can provide further insight concerning the feedback mechanisms

and the non-regulatory part of the network. However, further work is needed to differentiate between feedback mechanisms and the non-regulatory part of the network. Although, the exploratory analysis suggested in the chapter appears to be useful enough to identify unexpected correlations, we have noted that due to normalization methods used in this chapter we may lose some of the of the true negative correlations.

5 Conclusion

The C-SHIFT algorithm we have developed has been shown to effectively recover the empirical correlation structure that becomes obscured by technical noise. It does so much better than all other normalization methods that seem to produce normally distributed correlations no matter the true underlying distribution. However, for very small amounts of noise (where the observed correlation structure is virtually unchanged) the algorithm may sometimes create less accurate results. Detecting when this is the case is a future goal. Additionally, while in virtually all cases the Frobenius norm and trace objective function versions of the algorithm produce almost exactly the same estimates, there are occasional situations (generally in small noise scenarios) where they do not. Understanding why the differences occur is another area of future work. Especially since the trace version demonstrates much improved computational efficiency.

The algorithm also shows promising results in relation to the statistical tests used to detect differential expression. However, there are scenarios where rank normalization produces the lowest error rates. Understanding how to predict when to use each method is a goal of future work.

In situations with more realistic levels of noise, quantile normalization also performed quite well. In fact, we find that this type of normalization can even improve error rates (under certain conditions) when there is no noise present.

We identified key assumptions that must hold for quantile normalization to, on average, increase the magnitude of the test statistics that are used to identify significant differential expression. We showed the explicit improvement for one class of data and showed improvement for a more broad class of data under our assumptions. However, we plan to prove that our assumptions are sufficient for quantile normalization to enhance the efficacy of the t-tests in general.

In chapter 4, we discussed a probabilistic monotonicity property as biological networks transit from one state to another. While assumptions related to causality, allowed due to monotonicity, cannot hold across all possible biological processes, they seem to represent common features of various biological systems, particularly those for which the sample space can be represented by a distributive lattice with a partial order.

The individual statistical tests on means and correlations with multiplicity corrections seem to be one useful concept by which we can assess the monotonicity property. However, further work is needed to differentiate between feedback mechanisms and the non-regulatory part of the network. Although, the exploratory analysis suggested in the chapter appears to be useful enough to identify unexpected correlations, we have noted that due to normalization we may lose some of the of the true negative correlations. In a future study, we shall apply C-SHIFT normalization and see how the results compare.

While here we focused only on assessing monotonicity, there is further interest in direct and sparse estimation of network structures under the monotonicity assumption. For a single state, the monotonicity of log gene expressions leads to

the FKG inequality and the multivariate total positivity of order 2 [36]. Thus, under this assumption, there is interest in estimating the sparse inverse covariance matrix of log gene expressions which has all non-positive off-diagonal elements. This estimation problem was beautifully solved in a paper by [60]. For further reference on this topic see also [40]. The estimation mirrors the graphical lasso developed by [26] that did not have this additional constraint. Interestingly, to add the FKG inequality, we can also modify the least angle regression introduced by [23] and obtain an estimate of the inverse covariance matrix using positive lasso estimation. An area of possible future work is to revisit the estimation problem (with or without 4.1) simultaneously with the normalization.

Finally, there is also interest in studying probabilistic systems that can allow transition of biological networks without the monotonicity property. One such proposal arises through Russo's formula [28] in the Lorentz lattice gas model [39]. This is another potential topic of future work.

Bibliography

[1] Dhammika Amaratunga and Javier Cabrera. Analysis of data from viral dna microchips. *Journal of the American Statistical Association*, 96(456):1161–1170, 2001.

[2] Francis Bach. Breaking the curse of dimensionality with convex neural networks. *The Journal of Machine Learning Research*, 18(1):629–681, 2017.

[3] Y. Benjamini and Y. Hochberg. Controlling the false discovery rate: a practical and powerful approach to multiple testing. *Journal of the Royal Statistical Society*, 57(1):289—300, 1995.

[4] Jacob Bien and Robert J Tibshirani. Sparse estimation of a covariance matrix. *Biometrika*, 98(4):807–820, 2011.

[5] Martin Bilban, Lukas K Buehler, Steven Head, Gernot Desoye, and Vito Quaranta. Normalizing dna microarray data. *Current Issues in Molecular Biology*, 4:57–64, 2002.

[6] Jan C Bioch. Dualization, decision lists and identification of monotone discrete functions. *Annals of Mathematics and Artificial Intelligence*, 24(1-4):69–91, 1998.

[7] Benjamin M Bolstad, Rafael A Irizarry, Magnus Åstrand, and Terence P. Speed. A comparison of normalization methods for high density oligonucleotide array data based on variance and bias. *Bioinformatics*, 19(2):185–193, 2003.

[8] Atul J Butte, Pablo Tamayo, Donna Slonim, Todd R Golub, and Isaac S Kohane. Discovering functional relationships between rna expression and chemotherapeutic susceptibility using relevance networks. *Proceedings of the National Academy of Sciences*, 97(22):12182–12186, 2000.

[9] Sanjay Chaudhuri, Mathias Drton, and Thomas S Richardson. Estimation of a covariance matrix with zeros. *Biometrika*, 94(1):199–216, 2007.

[10] Evgenia Chunikhina, Paul Logan, Yevgeniy Kovchegov, Anatoly Yambartsev, Debashis Mondal, and Andrey Morgun. The covariance shift (c-shift) algorithm for normalizing biological data. *submitted*, 2020.

[11] William J Conover and Ronald L Iman. Rank transformations as a bridge between parametric and nonparametric statistics. *The American Statistician*, 35(3):124–129, 1981.

[12] David R Cox and David V Hinkley. *Theoretical statistics*, volume 1. Chapman & Hall, London, 1974.

[13] David R Cox and Nanny Wermuth. Linear dependencies represented by chain graphs. *Statistical science*, pages 204–218, 1993.

[14] David Roxbee Cox and Nanny Wermuth. *Multivariate dependencies: Models, analysis and interpretation*. Chapman and Hall/CRC, 2014.

[15] Peng Ding, Zhi Geng, Wei Yan, and Xiao-Hua Zhou. Identifiability and estimation of causal effects by principal stratification with outcomes truncated by death. *Journal of the American Statistical Association*, 106(496):1578–1591, 2011.

[16] David L. Donoho. High-dimensional data analysis: The curses and blessings of dimensionality. In *AMS conference on Mathematical Challenges of the 21st Century*. Citeseer, 2000.

[17] Mathias Drton and Michael D Perlman. Model selection for gaussian concentration graphs. *Biometrika*, 91(3):591–602, 2004.

[18] Mathias Drton and Thomas S Richardson. Graphical methods for efficient likelihood inference in gaussian covariance models. *Journal of Machine Learning Research*, 9(May):893–914, 2008.

[19] Marek J Druzdzel and Max Henrion. Efficient reasoning in qualitative probabilistic networks. In *Proc. National Conference on Artificial Intelligence (Washington D.C., USA, 1993)*, pages 548–553, 1993.

[20] David Edwards. *Introduction to graphical modelling*. Springer Science & Business Media, 2012.

[21] Bradley Efron. Correlation and large-scale simultaneous significance testing. *Journal of the American Statistical Association*, 102(477):93–103, 2007.

[22] Bradley Efron. *Large-scale inference: empirical Bayes methods for estimation, testing, and prediction*, volume 1. Cambridge University Press, 2012.

[23] Bradley Efron, Trevor Hastie, Iain Johnstone, and Robert Tibshirani. Least angle regression. *The Annals of statistics*, 32(2):407–499, 2004.

[24] Jianqing Fan, Heng Peng, and Tao Huang. Semilinear high-dimensional model for normalization of microarray data: a theoretical analysis and partial consistency. *Journal of the American Statistical Association*, 100(471):781–796, 2005.

[25] C. M. Fortuin, P. W. Kasteleyn, and J. Ginibre. Correlation inequalities on some partially ordered sets. *Communications in Mathematical Physics*, 22(2):89—-103, 1971.

[26] Jerome Friedman, Trevor Hastie, and Robert Tibshirani. Sparse inverse covariance estimation with the graphical lasso. *Biostatistics*, 9(3):432–441, 2008.

[27] Alexander N Gorban and Ivan Yu Tyukin. Blessing of dimensionality: mathematical foundations of the statistical physics of data. *Philosophical Transactions of the Royal Society A: Mathematical, Physical and Engineering Sciences*, 376(2118):20170237, 2018.

[28] G Grimmett. Percolation springer-verlag. *Berlin (Second edition)*, 1999.

[29] Michel Grzebyk, Pascal Wild, and Dominique Chouanière. On identification of multi-factor models with correlated residuals. *Biometrika*, 91(1):141–151, 2004.

[30] Alexander J Hartemink, David K Gifford, Tommi S Jaakkola, and Richard A Young. Using graphical models and genomic expression data to statistically validate models of genetic regulatory networks. In *Biocomputing 2001*, pages 422–433. World Scientific, 2000.

[31] Alexander J Hartemink, David K Gifford, Tommi S Jaakkola, and Richard A Young. Maximum-likelihood estimation of optimal scaling factors for expression array normalization. In *Microarrays: Optical Technologies and Informatics*, volume 4266, pages 132–140. International Society for Optics and Photonics, 2001.

[32] Paul W Holland and Paul R Rosenbaum. Conditional association and unidimensionality in monotone latent variable models. *The Annals of Statistics*, pages 1523–1543, 1986.

[33] Jessica Xin Hu, Cecilia Engel Thomas, and Søren Brunak. Network biology concepts in complex disease comorbidities. *Nature Reviews Genetics*, 17(10):615–629, 2016.

[34] Jianhua Hu and Xuming He. Enhanced quantile normalization of microarray data to reduce loss of information in gene expression profiles. *Biometrics*, 63(1):50–59, 2007.

[35] Paul C Kainen. Utilizing geometric anomalies of high dimension: When complexity makes computation easier. In *Computer Intensive Methods in Control and Signal Processing*, pages 283–294. Springer, 1997.

[36] Samuel Karlin and Yosef Rinott. Classes of orderings of measures and related correlation inequalities. I. Multivariate totally positive distributions. *Journal of Multivariate Analysis*, 10(4):467–498, 1980.

[37] MG Kendall and A Stuart. *The Advanced Theory of Statistics, Volume 2: Inference and Relationship*. Griffin, London, 1973.

[38] Kshitij Khare, Bala Rajaratnam, et al. Wishart distributions for decomposable covariance graph models. *The Annals of Statistics*, 39(1):514–555, 2011.

[39] Yevgeniy Kovchegov. Russo's formula for Lorentz Lattice Gas model. Technical report, Oregon State University, 2010.

[40] Steffen Lauritzen, Caroline Uhler, and Piotr Zwiernik. Maximum likelihood estimation in gaussian models under total positivity. *arXiv preprint arXiv:1702.04031*, 2017.

[41] H. B. Mann and D. R. Whitney. On a test of whether one of two random variables is stochastically larger than the other. *Annals of Mathematical Statistics*, 18(1):50–60, 1947.

[42] K. L. Mine, N. Shulzhenko, A. Yambartsev, M. Rochman, G. F. Sanson, M. Lando, S. Varma, J. Skinner, N. Volfovsky, T. Deng, S. M. Brenna, C. R. Carvalho, J.C. Ribalta, M. Bustin, P. Matzinger, I. D. Silva, H. Lyng, M. Gerbase-DeLima, and A. Morgun. Gene network reconstruction reveals

cell cycle and antiviral genes as major drivers of cervical cancer. *Nature Communications*, 2013.

[43] J. L. Myers and A. D. Well. *Research Design and Statistical Analysis*. Lawrence Erlbaum, Mahwah, NJ, 2nd edition, 2003.

[44] Taesung Park, Sung-Gon Yi, Sung-Hyun Kang, SeungYeoun Lee, Yong-Sung Lee, and Richard Simon. Evaluation of normalization methods for microarray data. *BMC Bioinformatics*, 4(1):33, 2003.

[45] Judea Pearl. *Causality*. Cambridge university press, Cambridge, England, 2009.

[46] Rob Potharst and Adrianus Johannes Feelders. Classification trees for problems with monotonicity constraints. *ACM SIGKDD Explorations Newsletter*, 4(1):1–10, 2002.

[47] Sylvain Pradervand, Johann Weber, Jérôme Thomas, Manuel Bueno, Pratyaksha Wirapati, Karine Lefort, G Paolo Dotto, and Keith Harshman. Impact of normalization on mirna microarray expression profiling. *RNA*, 15(3):493–501, 2009.

[48] Xing Qiu, Hulin Wu, and Rui Hu. The impact of quantile and rank normalization procedures on the testing power of gene differential expression analysis. *BMC Bioinformatics*, 14(1):124, 2013.

[49] J. Quackenbush. Microarray data normalization and transformation. *Nature Genetics*, 32:496–501, 2002.

[50] John Quackenbush. Microarray data normalization and transformation. *Nature Genetics*, 32(4):496–501, 2002.

[51] Miloš Radovanović, Alexandros Nanopoulos, and Mirjana Ivanović. Hubs in space: Popular nearest neighbors in high-dimensional data. *Journal of Machine Learning Research*, 11(Sep):2487–2531, 2010.

[52] N. A. Rahman. *A Course in Theoretical Statistics*. Hafner Press, London, 1968.

[53] Youlan Rao, Yoonkyung Lee, David Jarjoura, Amy S Ruppert, Chang-gong Liu, Jason C Hsu, and John P Hagan. A comparison of normalization techniques for microrna microarray data. *Statistical applications in genetics and molecular biology*, 7(1), 2008.

[54] Hans Reichenbach. *The direction of time*, volume 65. Univ of California Press, Berkeley, CA, 1991.

[55] Cavan Reilly, Changchun Wang, and Mark Rutherford. A method for normalizing microarrays using genes that are not differentially expressed. *Journal of the American Statistical Association*, 98(464):868–878, 2003.

[56] Edoardo Saccenti. Correlation patterns in experimental data are affected by normalization procedures: consequences for data analysis and network inference. *Journal of Proteome Research*, 16(2):619–634, 2017.

[57] Andreas Scherer. *Batch effects and noise in microarray experiments: sources and solutions*. John Wiley & Sons, 2009.

[58] L. Scotto, G. Narayan, S. V. Nandula, H. Arias-Pulido, S. Subramaniyam, A. Schneider, A. M. Kaufmann, J. D. Wright, B. Pothuri, M. Mansukhani, and V. V. Murty. Identification of copy number gain and overexpressed genes on chromosome arm 20q by an integrative genomic approach in cervical cancer: Potential role in progression. *Genes, Chromosomes, and Cancer*, 47(9):755–765, 2008.

[59] Zbynek Sidak, Pranab K Sen, and Jaroslav Hajek. *Theory of rank tests*. Academic press, San Diego, CA, 1999.

[60] Martin Slawski and Matthias Hein. Estimation of positive definite M-matrices and structure learning for attractive Gaussian Markov random fields. *Linear Algebra and its Applications*, 473:145–179, 2015.

[61] Gordon K Smyth and Terry Speed. Normalization of cdna microarray data. *Methods*, 31(4):265–273, 2003.

[62] Linda C van der Gaag, Hans L Bodlaender, and Ad Feelders. Monotonicity in Bayesian networks. In *Proceedings of the 20th conference on Uncertainty in artificial intelligence*, pages 569–576. AUAI Press, 2004.

[63] Tyler J VanderWeele and James M Robins. Signed directed acyclic graphs for causal inference. *Journal of the Royal Statistical Society: Series B (Statistical Methodology)*, 72(1):111–127, 2010.

[64] YX Rachel Wang and Haiyan Huang. Review on statistical methods for gene network reconstruction using expression data. *Journal of theoretical biology*, 362:53–61, 2014.

[65] B. L. Welch. The generalization of "Student's" problem when several different population variances are involved. *Biometrika*, 34(1/2):28–35, 1947.

[66] Michael P Wellman. Graphical inference in qualitative probabilistic networks. *Networks*, 20(5):687–701, 1990.

[67] A. Yambartsev, M. Perlin, Y. Kovchegov, N. Shulzhenko, K. L. Mine, X. Dong, and A. Morgun. Unexpected links reflect the noise in networks. *Biology Direct*, 11, 2016.

APPENDIX

A Empirical Null Modeling

Efron [21] first showed that the covariance matrix of binned counts of z-values (converted p-values) could be split into the sum of an independence term, C_0 (covariance if all tests are independent), and a term that accounts for the dependence, C_1. If the vector of counts is b and the $E[b] = d$ then

$$
\begin{aligned}
\mathrm{Cov}(b_k, b_l) &= \mathrm{E}[b_k b_l] - \mathrm{E}[b_k]\,\mathrm{E}[b_l] \\
&= \mathrm{E}\left[\sum_{i,j} I(z_i \in \mathrm{bin}_k) I(z_j \in \mathrm{bin}_l)\right] \\
&\qquad - \mathrm{E}\left[\sum_{i} I(z_i \in \mathrm{bin}_k)\right] \mathrm{E}\left[\sum_{j} I(z_j \in \mathrm{bin}_l)\right] \\
&= \mathrm{E}\left[\sum_{i \neq j} I(z_i \in \mathrm{bin}_k) I(z_j \in \mathrm{bin}_l)\right] \\
&\qquad - \mathrm{E}\left[\sum_{i} I(z_i \in \mathrm{bin}_k)\right] \mathrm{E}\left[\sum_{j} I(z_j \in \mathrm{bin}_l)\right] \\
&= \sum_{i \neq j} Pr(z_i \in \mathrm{bin}_k, z_j \in \mathrm{bin}_l) - m^2\,\mathrm{E}[b_k]\,\mathrm{E}[b_l] \\
&= \sum_{i \neq j} Pr(z_i \in \mathrm{bin}_k, z_j \in \mathrm{bin}_l) - d_k d_l + d_k d_l/m - d_k d_l/m \\
&= d_k d_l/m + \left[\sum_{i \neq j} Pr(z_i \in \mathrm{bin}_k, z_j \in \mathrm{bin}_k) - m(m-1) d_k d_l/m^2\right] \\
&= d_k d_l/m + \left(1 - \frac{1}{m}\right) d_k \delta_{kl} d_l
\end{aligned}
$$

where m is the number of tests and

$$\delta_{kl} = \frac{m^2}{m(m-1)} \frac{\sum_{i \neq j} Pr(z_i \in \text{bin}_k, z_j \in \text{bin}_l)}{d_k d_l} - 1 \ .$$

Similarly,

$$\begin{aligned}
\text{Cov}(b_k, b_k) &= \text{E}[b_k^2] - (\text{E}[b_k])^2 \\
&= \text{E}\left[\sum_{i,j} I(z_i \in \text{bin}_k) I(z_j \in \text{bin}_k)\right] - \text{E}^2\left[\sum_i I(z_i \in \text{bin}_k)\right] \\
&= \text{E}\left[\sum_i I(z_i \in \text{bin}_k)\right] + \text{E}\left[\sum_{i \neq j} I(z_i \in \text{bin}_k) I(z_j \in \text{bin}_k)\right] \\
&\quad - \text{E}^2\left[\sum_i I(z_i \in \text{bin}_k)\right] \\
&= \text{E}[b_k] + \sum_{i \neq j} Pr(z_i \in \text{bin}_k, z_j \in \text{bin}_k) - m^2 \, \text{E}^2[b_k] \\
&= d_k + \sum_{i \neq j} Pr(z_i \in \text{bin}_k, z_j \in \text{bin}_k) - d_k^2 + d_k^2/m - d_k^2/m \\
&= d_k - d_k^2/m + \left[\sum_{i \neq j} Pr(z_i \in \text{bin}_k, z_j \in \text{bin}_k) - m(m-1) d_k^2/m^2\right] \\
&= d_k - d_k^2/m + \left(1 - \frac{1}{m}\right) d_k \delta_{kk} d_k \ .
\end{aligned}$$

Thus, we find that

$$\text{Cov}(b) = C_0 + C_1$$

with

$$C_0 = \text{diag}(d) - dd^T/m \quad \text{and} \quad C_1 = \left(1 - \frac{1}{m}\right) \text{diag}(d)\delta \,\text{diag}(d) \ .$$

If $z[b_k]$ is the center point of the kth bin and Δ is the bin width, then d_k can be expressed as $d_k = m\Delta\phi(z[b_k])$ where $\phi(z[b_k])$ is the standard normal pdf at $z[b_k]$. By assuming that any pair of z-values would have approximately a bivariate normal distribution, $\text{Cov}(z_i, z_j) = \rho_{ij}$, and that the empirical density of correlations, $g(\rho)$, has mean zero and standard deviation $\alpha = \left[\int_{-1}^{1} \rho^2 g(\rho) d\rho\right]^{1/2}$, Efron was able to derive an expression for δ_{kl} in terms of the bin center points and α. Specifically,

$$\delta_{kl} = \alpha^2 \ \frac{z[b_k]^2 - 1}{\sqrt{2}} \ \frac{z[b_l]^2 - 1}{\sqrt{2}} \ .$$

Therefore, if we define $W_k = m\Delta(z[b_k]^2 - 1)\phi(z[b_k])/\sqrt{2}$ as the components of the vector W and note that

$$W_k W_l = m^2\Delta^2 \frac{(z[b_k]^2 - 1)\phi(z[b_k])}{\sqrt{2}} \frac{(z[b_l]^2 - 1)\phi(z[b_l])}{\sqrt{2}} = d_k \delta_{kl} d_l/\alpha^2$$

then

$$\text{Cov}(b) \ \doteq \ [\text{diag}(d) - dd^T/m] + \left(1 - \frac{1}{m}\right)(\alpha W)(\alpha W)^T.$$

Of course, with a very large number of tests, m, this can be simplified to

$$\text{Cov}(b) \ \doteq \ \text{diag}(d) + (\alpha W)(\alpha W)^T.$$

He then utilized a Poisson hierarchical model (conditioned on the parameter A related to the dependence) to achieve the desired expectation vector and covariance matrix.

$$b|A \sim Poisson(d + AW), \quad \text{with} \quad A \sim (0, \alpha^2)$$

While the components of b are dependent, the conditional components of $b|A$ are independent. The desired results can be confirmed by using the Laws of Total Expectation and Variance as shown.

$$\mathrm{E}[b] = \mathrm{E}[\mathrm{E}[b|A]] = \mathrm{E}[d + AW] = d$$

$$\begin{aligned} \mathrm{Cov}(b) &= \mathrm{E}[\mathrm{Cov}(b|A)] + \mathrm{Cov}(\mathrm{E}[b|A]) \\ &= \mathrm{E}[\mathrm{diag}(d + AW)] + \mathrm{Cov}(d + AW) \\ &= \mathrm{diag}(d) + (\alpha W)(\alpha W)^T \end{aligned}$$

Next Efron summed the conditional bin counts, $\mathrm{E}[b|A]$, in the tails and took the limit as the bin size went to 0. Thus, the expected number of z-values in the tails under the null would be

$$\begin{aligned} \mathrm{E}\left[\sum_i H_0 : \ z_i \geq x|A\right] &= m[1 - \Phi(x)] + mA\frac{x\phi(x)}{\sqrt{2}} \\ &= m[1 - \Phi(x)]\left(1 + \frac{A}{\sqrt{2}}\frac{x\phi(x)}{[1 - \Phi(x)]}\right) \end{aligned}$$

where Φ is the standard normal distribution function. By scaling the expected

tail counts under the null by the true tail counts, he achieved an estimate of the conditional FDR as a function of the individual z-scores. However, an estimate for A is still needed. Efron proposed using a proportion of the central z-scores to estimate it in the following way. Specifically, we let

$$z_i = \Phi^{-1}\left(1 - p_i^{(1)}\right) \quad \text{and} \quad \hat{A} = \frac{P_0 - \hat{P}_0}{Q_0},$$

where

$$P_0 = 2\ \Phi(z_0) - 1, \qquad Q_0 = \sqrt{2}\ z_0\ \phi(z_0), \qquad \hat{P}_0 = \frac{1}{m}\sum_i I(z_i \in [-z_0, z_0]).$$

Obviously, z_0 controls the central proportion of the data used for the empirical null. A standard value proposed by Efron is $z_0 = 1$. Then,

$$p_{i,E}^{(1)} = FDR_0(z_i)\left[1 + \hat{A}\frac{z_i\phi(z_i)}{\sqrt{2}(1 - \Phi(z_i))}\right],$$

is effectively an adjusted p-value, where $FDR_0(z_i) = N(1 - \Phi(z_i))/\left(\sum_j z_j \geq z_i\right)$ would be the unconditioned (ie, assuming independence) estimate of the FDR under the null hypothesis.